INFRARED, RAMAN, AND LUMINESCENCE SPECTRA OF PHENYL ISOCYANIDE AND PERDEUTEROPHENYL ISOCYANIDE

INFRARED, RAMAN, AND LUMINESCENCE SPECTRA OF PHENYL ISOCYANIDE AND PERDEUTEROPHENYL ISOCYANIDE

by

ROBERT ALLAN NALEPA, B.Sc.

A Thesis

Submitted to the School of Graduate Studies

in Partial Fulfilment of the Requirements

for the Degree

Master of Science

McMaster University

November 1973

MASTER OF SCIENCE

(Chemistry)

McMASTER UNIVERSITY

Hamilton, Ontario

TITLE: Infrared, Raman, and Luminescence Spectra of Phenyl Isocyanide and Perdeuterophenyl Isocyanide

AUTHOR: Robert Allan Nalepa, B.Sc. (Saint Francis Xavier University)

SUPERVISOR: Dr. Joseph D. Laposa

NUMBER OF PAGES: ix, 111

ACKNOWLEDGMENTS

I would like to express my appreciation and gratitude to Dr. J. D. Laposa, my research supervisor, for his thoughtfulness, understanding, and assistance during the course of my research and thesis preparation.

I would also like to thank my fellow graduate students; Hal Singh, Vince Morrison and Dave Condirston for their help and companionship.

Many thanks go out to the Excited States, especially "The Blanket".

I am also grateful to Mrs. Louise Van Thielen for recording the Raman Spectra, to Dr. R. A. Bell and Mrs. C. Chan for preparation of the isocyanides, and to the Chemistry Department for financial assistance.

I wish also to thank Miss Lydea de Jong for her patience and excellent typing.

Finally, I wish to thank all the friends I made at McMaster for making my stay here an enjoyable one.

TABLE OF CONTENTS

LIST OF ILLUSTRATIONS

LIST OF TABLES

TO MY MOTHER AND FATHER

CHAPTER I

INTRODUCTION

Molecular spectroscopy is concerned with the interaction of an electromagnetic radiation field with an ensemble of molecules.

Such studies yield much useful information such as dipole moments, various quantized energies associated with a molecule, force constants of the bonds between the atoms of a molecule, normal vibrational frequencies which may be used to compute thermodynamic quantities, and molecular structure.

Molecular structure refers to the relative positions of the nuclei of a molecule at vibrational equilibrium. In general the geometrical structures of the ground and excited electronic states differ. The structure of the ground electronic state has been determined for many simple polyatomics through infrared spectra which give the normal vibrational frequencies and force constants between atoms; microwave spectra which give rotational constants which in turn allow one to calculate moments of inertia and hence bond lengths, and electron diffraction studies which allow one to calculate bond distances and angles.

In contrast, structures are known for very few excited electronic states. Occasionally the rotational fine structure of a vibronic band in an electronic absorption system is well enough resolved to permit the calculation of the rotational constants and hence geometry of the excited

electronic state. If the rotational structure is not well enough resolved one may be able to obtain information on the structure of the excited state by observing a series of sub-bands or the shape of the band envelope.

The only alternative method of gaining information about the structure of an electronic excited state is via the Franck-Condon principle. This principle states that the most probable vibronic transition is one for which there is no change in nuclear configuration. This holds true for both absorption and emission. Emission studies, phosphorescence in particular, are important because they yield information about the geometry of the lowest triplet state when in some cases direct absorption from the ground singlet state to the lowest triplet state is very weak or not seen at all due to the spin forbiddenness of the transition. The Franck-Condon principle has been quantitatively applied to the determination of electronic state geometry changes by relative intensity measurements on the members of a progression for both absorption data[1,2] and emission data[3]. Qualitatively from the Franck-Condon principle, if two electronic states involved in a transition differ in geometry then one observes a progression or progressions in the normal vibration or vibrations which convert the geometry of one state into the other. The most prominent progression will be in that vibration with respect to the normal coordinate whose equilibrium value is most greatly changed by the electronic transition.

The work reported here involved the infrared and Raman studies of phenyl isocyanide and perdeuterophenyl isocyanide so as to determine

their normal modes of vibration which were then used to make assignments in the luminescence spectra of these molecules. Their luminescence spectra were recorded in rigid polycrystalline matrices at 77°K.

The luminescence and vibrational spectra of two molecules isoelectronic with phenyl isocyanide, namely, ethynylbenzene[4,5,6] and benzonitrile[7,8,9] were previously studied and so it was of interest to find out how phenyl isocyanide behaved compared to the other two molecules spectroscopically.

The Franck-Condon principle was applied qualitatively in this work in the determination of the geometry of the first excited singlet electronic state and lowest triplet state for both molecules. The first excited singlet state of benzene has been shown to be slightly expanded and hexagonal[1] and to be hexagonal[10] or nearly so[3,11,12] in the lowest triplet state. It is of interest to note the geometrical changes, if any, in these states by substitution of H by - N $\overset{+}{=}$ C.

Although the ground state geometry of phenyl isocyanide is unknown, it will be assumed here, as by Muirhead et al[13] that the molecule is planar and belongs to the C_{2V} point group.

There has been little previous spectroscopic work on phenyl isocyanide. A solution spectrum of phenyl isocyanide was obtained by Wolf and Strasser[14]. An infrared spectrum of phenyl isocyanide as a film in the 4000 - 667 cm^{-1} region was reported by Ugi and Meyr[15] but no vibrational analysis was attempted. More recently, in the gas phase ultraviolet absorption and gas phase infrared studies of Muirhead et al[13] an attempt was made to assign a few vibrational frequencies

of C_6H_5NC. No infrared spectrum was shown in their paper. No mention of perdeuterophenyl isocyanide, C_6D_5NC, has been found in the literature. Likewise, luminescence work of either C_6H_5NC or C_6D_5NC has not been reported in the literature.

Polarization data obtained by the method of photoselection was used to assign the orbital symmetry of the lowest excited triplet state.

Phosphorescence lifetimes of C_6H_5NC and C_6D_5NC in various solvents were also determined.

CHAPTER II

THEORY

2.1 Symmetry Classification of Phenyl Isocyanide

If the symmetry elements possessed by an isolated molecule in its equilibrium nuclear configuration are examined, one is able to assign that molecule to a specific symmetry point group.

Although the ground state geometry of phenyl isocyanide has not been determined, it is assumed in this work as by Muirhead et al[13] to be planar with the substituent group, -N ≡ C, lying on a straight line bisecting the benzene ring.

Phenyl isocyanide as well as perdeuterophenyl isocyanide has three symmetry elements in addition to the identity element. These symmetry elements are a two-fold rotation axis and two reflection planes. These symmetry elements are shown in Figure 2.1, in which the coordinate axes have been defined according to Mulliken's convention[16]. The corresponding symmetry operations are:

$C_2(z)$, rotation about the z-axis through 180°;

$\sigma_v(xz)$, reflection in a plane perpendicular to the molecular plane;

$\sigma_v'(yz)$, reflection in the molecular plane.

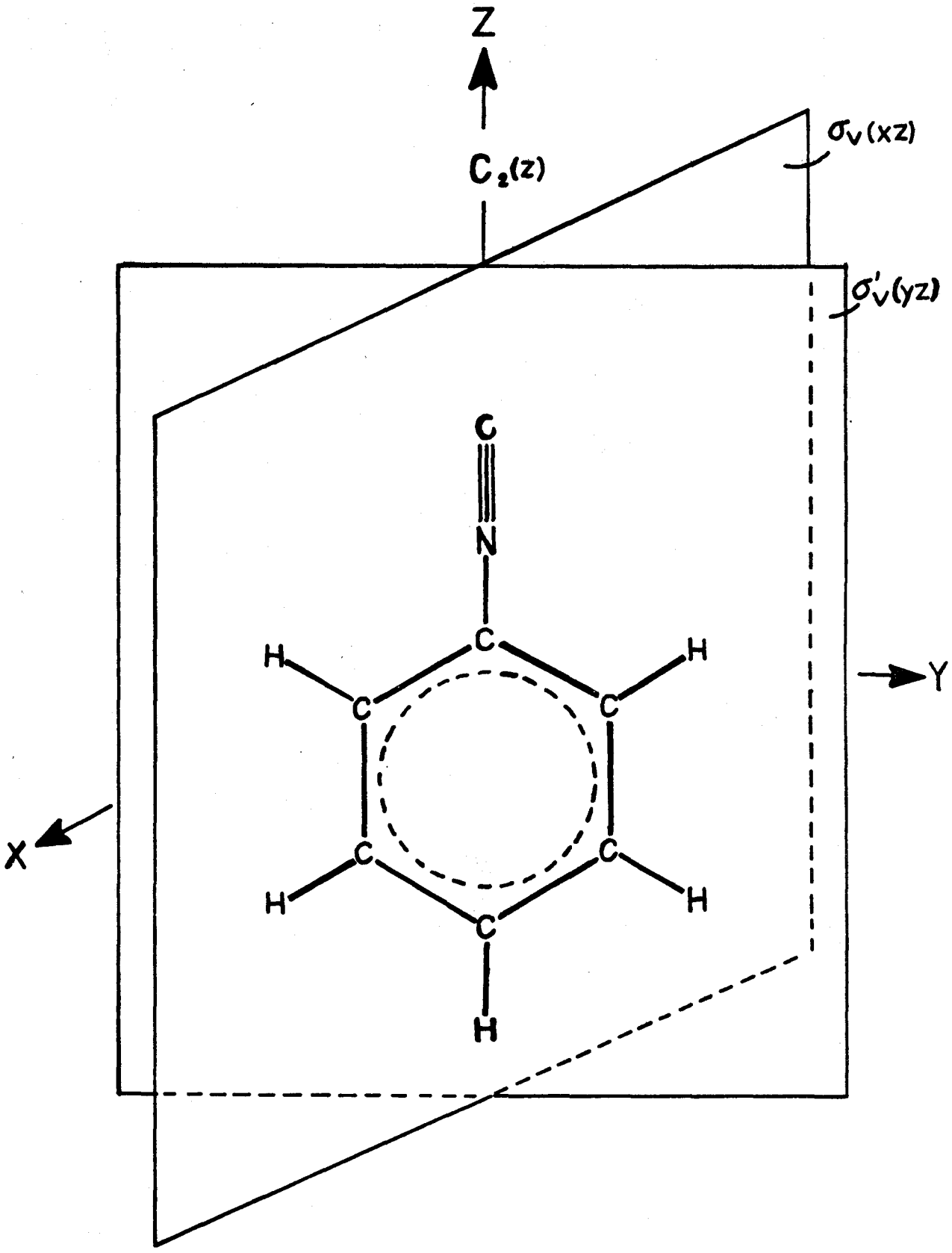

Figure 2.1 Symmetry Elements of Phenyl Isocyanide.

TABLE 2.1

Character Table of the C_{2V} Point Group

C_{2V}	E	$C_2(z)$	$\sigma_V(xz)$	$\sigma'_V(yz)$			
A_1	1	1	1	1	z		x^2, y^2, z^2
A_2	1	1	-1	-1		R_z	xy
B_1	1	-1	1	-1	x	R_y	xz
B_2	1	-1	-1	1	y	R_x	yz

TABLE 2.2

Direct Product Table of the C_{2V} Point Group

C_{2V}	A_1	A_2	B_1	B_2
A_1	A_1	A_2	B_1	B_2
A_2	A_2	A_1	B_2	B_1
B_1	B_1	B_2	A_1	A_2
B_2	B_2	B_1	A_2	A_1

These three symmetry operations together with the identity operation E constitute the C_{2v} point group to which the phenyl isocyanide and perdeuterophenyl isocyanide molecules belong.

The character and direct product tables of the C_{2v} point group are given in Tables 2.1 and 2.2. They are of use in determining which vibrational modes are Raman and infrared active, and which electronic transitions are symmetry allowed.

2.2 The Born-Oppenheimer Approximation

The time-independent Schrodinger equation for an isolated molecule is given by:

$$H \psi_t = E_t \psi_t \qquad (2.1)$$

where E_t represents the total internal energy of the molecule, that is, the sum of the kinetic energy and the potential energy of all the electrons and nuclei present. ψ_t represents a stationary state of the molecule and is a function of the coordinates of all the electrons and nuclei. H is known as the Hamiltonian operator and consists of the kinetic energy operator of the electrons (T_e) and the nuclei (T_n), plus the potential energy operators for the coulombic interactions between electrons (V_{ee}), nuclei (V_{nn}), and finally electrons and nuclei (V_{en}) . Thus if one neglects the translation of the molecule as a whole and also neglects spin and relativistic

effects, the Hamiltonian, H, is written as:

$$H = (K.E. + P.E.) = T_e + T_n + V_{ee} + V_{nn} + V_{en} \cdot \qquad (2.2)$$

The detailed form of the above operators may be found in reference (17).

Since the masses of the nuclei are much greater than the mass of the electron and hence move much more slowly, Born and Oppenheimer[18] were able to show that to a good approximation the complete wave function ψ_t can be written as a product of the electronic wave function ψ_e and the nuclear wave function ψ_n, that is:

$$\psi_t = \psi_e \psi_n \cdot \qquad (2.3)$$

Thus an approximate solution of the complete wave equation for a molecule can be obtained by first solving the wave equation for the electrons alone,

$$H_e\psi_e = E_e\psi_e \ , \qquad (2.4)$$

where

$$H_e = T_e + V_{ee} + V_{en} \qquad (2.5)$$

with the nuclei in a fixed configuration (i.e., with $T_n = 0$ and V_{nn} = constant), and then solving a wave equation (2.6) for the nuclei alone, in which the energy value E_e of the electronic wave equation (2.4), regarded as a function of the internuclear distances, occurs as a potential function.

$$(T_n + V_{nn} + E_e)\ \psi_n = E\ \psi_n \qquad (2.6)$$

The Born-Oppenheimer approximation is valid providing the electronic wave function is not a rapidly changing function of the nuclear coordinates.

The motion of a molecule can be separated into three types: electronic, vibrational, and rotational. If one assumes that because of the different time factors involved with each type of motion there is little interaction between them, then to a good approximation the total wave function may be written as:

$$\psi_t = \psi_e\ \psi_v\ \psi_r \quad . \qquad (2.7)$$

The total energy of the molecule may then be written as the sum of the energies associated with each particular type of motion:

$$E_t = E_e + E_v + E_r \quad . \qquad (2.8)$$

2.3 Spectroscopic Transitions

In order for a molecule to undergo a spectroscopic transition, i.e., absorption or emission between two states of energy E_1 and E_2, the absolute value of the difference in energy between these two states must be equal to $h\nu$. Put in equation form:

$$|E_1 - E_2| = h\nu \quad . \qquad (2.9)$$

More commonly, one sees the above equation presented as:

$$\bar{\nu} = \frac{|E_1 - E_2|}{hc} \qquad (2.10)$$

where $\bar{\nu}$ is the frequency of the electromagnetic radiation absorbed or emitted, expressed in cm^{-1} and also equivalent to the reciprocal of the wavelength λ; E_1, E_2 are the energies of the two states in ergs; h is Planck's constant, which is equal to 6.62×10^{-27} erg-sec; and c is the speed of light in vacuum, having a value of 3.00×10^{10} cm sec^{-1}.

2.4 Classification of Electronic States for Polyatomic Molecules

Electronic states are first classified with respect to multiplicity or spin degeneracy and also with respect to symmetry.

The former classification leads to singlet, doublet, triplet, etc., terms. Accordingly the states are assigned a superscript to the left upper corner of the symbol for the state, this superscript being equal to the value of 2S + 1, where S is the total electronic spin quantum number.

Each unpaired electron in the molecule contributes a value of 1/2 to S. If the total number of electrons in the molecule is even and all the electrons in the molecule are paired, that is, have spins which are antiparallel, then the resultant value of S is 0 and the state is designated as a singlet. Most aromatic hydrocarbons have a singlet ground state. If the

spins of all the electrons of a molecule are paired except for two molecular orbitals containing a single electron each, whose spins are parallel, then that electronic state is classified as a triplet.

For atoms or linear molecules one may specify a state symmetry by considering the angular momenta of the system about a naturally preferential direction such as the internuclear axis. However, for non-linear polyatomics one cannot find a naturally preferential direction and thus cannot define meaningful angular momenta for the whole system. In this case the electronic state classification is based on the transformation properties of their wave functions under the symmetry operations of the point group, to which the molecule belongs. This classification is based on the assumption that the nuclei are fixed in their equilibrium positions and still holds as long as the symmetry of the displaced nuclei is that of the equilibrium nuclei.

Thus for the phenyl isocyanide and perdeuterophenyl isocyanide, one is able to determine the symmetry of all its possible electronic states by looking up the irreducible representations of the C_{2V} point group as found in a character table such as Table 2.1. These irreducible representations correspond to various electron configurations for the molecule. By knowing in which molecular orbitals the electrons are located and their corresponding symmetry the symmetry of the electronic state for the system may be determined by taking a direct product of the occupied orbitals. From the character table one sees that the possible classification of states for these molecules are A_1, A_2, B_1 and B_2.

2.5 Theory of Infrared Spectra

A brief summary of the theory of vibrational spectra is presented here. A detailed treatment of this topic can be found in references (17), (19) and (20).

A molecule may be considered as a semi-rigid body with its nuclei as point masses. These nuclei are coupled as a result of electrostatic interactions between the nuclei and electrons.

A non-linear N-atomic molecule has 3N-6 vibrational degrees of freedom or normal modes associated with it. The characteristics of a normal mode are that each atom reaches its position of maximum displacement at the same time, and each atom passes through its equilibrium position at the same time.

The phenyl isocyanide and perdeuterophenyl isocyanide molecules are both of C_{2V} symmetry. Each normal vibration can be assigned a symmetry species which describes an irreducible representation of the molecular point group. The characters of the representation spanned by the 3N-6 = 33 vibrational normal modes or coordinates of these molecules are calculated to be:

	E	$C_2(z)$	$\sigma_V(xz)$	$\sigma_V'(yz)$
X[Γ(ViB)]:	33	-3	5	13

This representation, upon decomposition, gives the following direct sum of irreducible representations:

$$\Gamma(ViB) = 12A_1 + 3A_2 + 7B_1 + 11B_2 \quad . \qquad (2.11)$$

The 33 normal vibrations of phenyl isocyanide and perdeuterophenyl isocyanide therefore consist of $12A_1$, $3A_2$, $7B_1$ and $11B_2$ symmetry species.

Although there are 3N-6 possible fundamental vibrations for a non-linear polyatomic molecule, only those which cause a change in the dipole moment will be infrared active.

A molecule is considered in its ground vibrational level when all the vibrational quantum numbers V_i are zero. This ground level is totally symmetric and non-degenerate. A band for which the vibrational quantum number V_j has a value of 1 and all other V_i have a value of 0 is called a fundamental of the jth vibration. Besides fundamental bands, overtones and combination bands may be seen but are generally weaker than the fundamental bands. Overtone bands are multiples of a fundamental and combination bands are sums or differences of fundamentals.

Each vibration of the molecule is approximated as that of a harmonic oscillator, whose energy levels are given by:

$$E_i = (V_i + 1/2)\, h\nu_i \qquad (2.12)$$

where V_i is the quantum number which can take on any positive integral value including zero, while ν_i is the classical frequency of the system; h is Planck's constant. Figure 2.2 shows the energy levels for a harmonic and

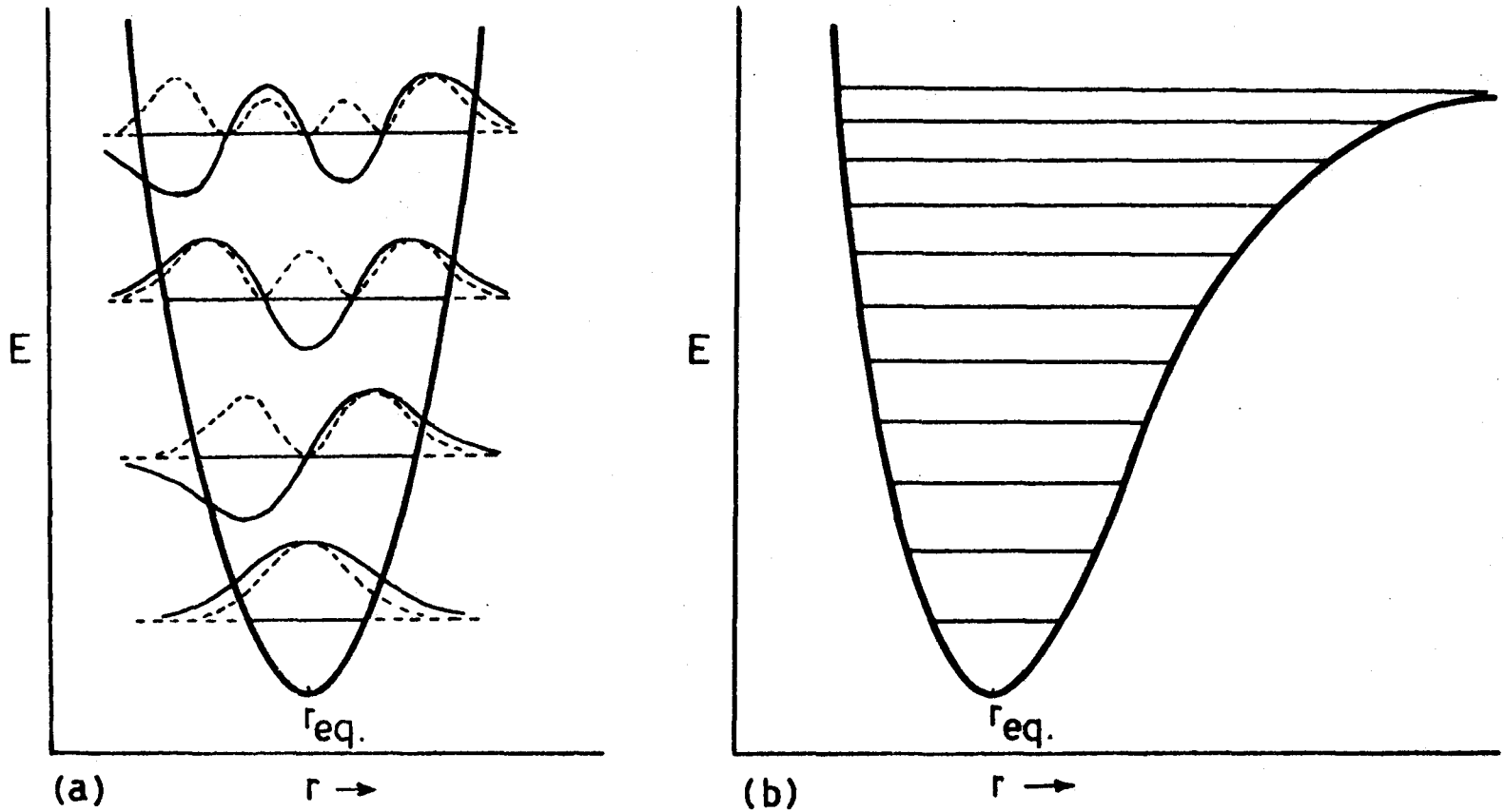

Fig. 2·2 Potential energy diagram with energy levels, eigenfunctions, and probability density distribution (---) for an harmonic (a) and anharmonic (b) oscillator.

anharmonic oscillator.

The vibrational wave function for the molecule, ψ_V, is expressed as a product of harmonic oscillator functions, one for each normal mode and the total vibrational energy of the molecule is given by:

$$E_V = (v_1+1/2)\ h\nu_1 + (v_2+1/2)\ h\nu_2 + ... + (v_{3N-6}+1/2)h\nu_{3N-6} \cdot \qquad (2.13)$$

The selection rule for the allowed vibrational transitions of a harmonic oscillator is:

$$\Delta V = \pm 1 \cdot \qquad (2.14)$$

The fact that overtones and combination bands are seen means that the molecule is not really vibrating as a harmonic oscillator but rather as a anharmonic oscillator and corrections for anharmonicity must be introduced into the equations of vibrational motion because the actual potential energy curves for molecules are not quadratic potential functions of the type which describe harmonic motion.

The quantum mechanical probability of a transition between two vibrational levels is proportional to the square of the vibrational transition moment:

$$R_{V'V''} = \langle \psi_{V'} \ |M|\ \psi_{V''} \rangle \qquad (2.15)$$

where $R_{V'V''}$ is the vibrational transition moment; $\psi_{V'}$, $\psi_{V''}$ are the wave

functions for the two vibrational states involved in the transition and M is the electric dipole moment operator having the form:

$$M = M_x + M_y + M_z = \Sigma_i \, er_i \qquad (2.16)$$

e being the charge of the electron and r_i the vector distance of the ith electron from an origin of a coordinate system fixed for the molecule. These components M_x, M_y and M_z transform as translations x, y, and z and are equivalent to B_1, B_2 and A_1 respectively under the C_{2V} point group.

Thus for a vibrational transition to be allowed between V' and V", the integral of $\psi_{V'} M \psi_{V''}$ must be non-zero. This will be the case only when there is at least one component of the dipole moment operator M that has the same species as the product $\psi_{V'}\psi_{V''}$. Therefore, for a molecule of C_{2V} symmetry B_1, B_2 and A_1 vibrations should be infrared active while A_2 vibrations are infrared inactive and thus should not appear in an infrared spectrum. However, it is found in this work, as in other infrared studies of monosubstituted benzenes, that a_2 fundamentals do appear, although weakly; this is presumably due to the perturbing effects of the liquid environment.

2.6 Isotope Effect

When an atom of a molecule is replaced by an isotopic atom of the same element, the potential energy function under the influence of which

the nuclei are moving and the configuration of the molecule are assumed to be changed by negligible amounts since isotopic molecules have the same electronic structure. However, because of the difference in the masses, the vibrational frequencies (levels) are different. There may be an appreciable difference in frequencies if there is a large change in mass involved, i.e., substituting deuterium for hydrogen. A study of the isotopic shifts will aid in a vibrational analysis of the molecule. The magnitude of the shift an isotope produces is indicative of the extent to which that particular atom participates in a vibration, provided no factors other than the change in mass are involved in the observed shift.

2.7 Teller-Redlich Product Rule

The Teller-Redlich Product Rule is a rule which relates for two isotopic molecules, the ratio of frequencies of all their vibrations of a given symmetry type.

For phenyl isocyanide $-h_5$ and $-d_5$ only the product ratio for the vibrational a_1 modes is given below because of the lack of moment of inertia data necessary to compute the product ratio for the other modes:

$$\pi_i \frac{\omega_i^D}{\omega_i^H} = \left(\frac{m^H}{m^D} \right)^2 \sqrt{\frac{m^H}{m^D} \cdot \frac{M^D}{M^H}} \qquad (2.17)$$

where the superscripts D and H refer to the values of C_6D_5NC and C_6H_5NC, respectively; m and M are the respective masses for the atom and molecule;

ω_i are the zero order frequencies.

The product rule holds rigorously for the zero-order frequencies ω_i and at least to a good approximation for the observed fundamentals ν_i for any mass difference.

2.8 Theory of Raman Spectra

A very brief treatment of the theory of Raman spectra is given here. A thorough treatment may be found in references (19), (21) and (22).

The Raman process is a light scattering and not an absorption phenomenon. The molecular interaction with the incident radiation is through the polarizability of the molecule and not through the dipole moment as is the case for infrared absorption. Thus the polarizability and not the dipole moment must change during a vibration in order for a vibration to be Raman active.

The scattered radiation, after the molecule has been irradiated with monochromatic light, is analyzed and it is the frequency shift of the bands from the exciting source frequency which is important rather than the absolute frequency of the scattered radiation. These frequency shifts correspond to the various vibrations of the molecule.

The selection rule for the vibrational changes in the Raman process is the same as for the infrared, i.e., $\Delta V = \pm 1$.

The vibrational transition moment for the Raman effect is given by:

$$P_{nm} = \langle \psi_m \alpha_{ij} \psi_n \rangle E \qquad (2.18)$$

where P_{nm} is the vibrational transition moment for the two vibrational states ψ_m and ψ_n; α_{ij} is the polarizability of the molecule, having six components which transform as xy, xz, yz, x^2, y^2 and z^2, and is regarded as a function only of the nuclear vibrational coordinates; E is the electric vector of the incident radiation. Thus, in order for a vibration to be Raman active, i.e., for the vibrational transition moment to be non-zero at least one component of the polarizability must be of the same species as the product $\psi_m\psi_n$. A quick glance at character Table 2.1 shows that for a C_{2V} molecule all the fundamental vibrations are Raman active, i.e., vibrations of A_1, A_2, B_1 and B_2 symmetry.

2.9 Depolarization Ratios

The depolarization ratio of a Raman band is defined as:

$$\rho = \frac{I_{\perp}}{I_{\parallel}} \qquad (2.19)$$

where $I_{\perp}$ and $I_{\parallel}$ are the intensities of the Raman bands polarized perpendicular and parallel to the plane of polarization of the incident radiation. This work was done with laser sources and thus the incident light is

plane-polarized. Therefore this ratio lies between 0 and 3/4 for totally symmetric vibrations which are then said to be polarized and is equal to 3/4 for non-totally symmetric vibrations which are said to be depolarized. Thus depolarization values are very useful in the vibrational analysis of a molecule.

2.10 Theory of Electronic Transitions

Most electronic transitions that take place give rise to spectra in the ultraviolet and visible regions of the electromagnetic spectrum. In contrast to spectra of gaseous molecules, it is typical of molecules in condensed phases to show an absorption which is broad and without structure or with only a few sub-bands.

Typical separation of electronic states is of the order of 10,000 cm^{-1}. This is to be compared to the separation of different vibrational and rotational levels belonging to a given electronic state of 1,000 and 10 - 100 cm^{-1} respectively[23].

For a pure electronic transition between upper and lower non-degenerate electronic states $\psi_{e'}$ and $\psi_{e''}$, the probability of the transition is given by the square of the electronic transition moment $R_{e'e''}$, where:

$$R_{e'e''} = \langle \psi_{e'} |M| \psi_{e''} \rangle \quad . \tag{2.20}$$

M is the electric dipole moment operator. Thus for a pure electronic

transition to be allowed the product $\psi_{e'}\psi_{e''}$ must transform as at least one of the components of M.

The above condition for a pure electronic transition to be allowed holds strictly for fixed nuclei. In real molecules nuclei are not fixed and therefore the total eigenfunction which includes the nuclear coordinates must be considered. Thus using the Born-Oppenheimer approximation to write the total eigenfunction (neglecting rotation) one obtains:

$$\psi_{ev} = \psi_e \cdot \psi_v = \psi_e\,(q, Q)\ \psi_v\,(Q) \qquad (2.21)$$

where q stands for all the electronic coordinates and Q for the nuclear coordinates. The wave function ψ_{ev} represents a vibronic state. When one writes ψ_{ev} as a simple product of ψ_e and ψ_v, the finer interaction of electronic motion and vibration must be neglected but that part of this interaction that can be expressed by the dependence of the electronic wave function ψ_e on the nuclear coordinates Q is retained[24].

The probability of an electric dipole transition between two non-degenerate vibronic levels $\psi_{e'v'}$ and $\psi_{e''v''}$ is proportional to the square of the transition moment integral $R_{e'v'e''v''}$:

$$R_{e'v'e''v''} = \langle \psi_{e'v'} \,|M|\, \psi_{e''v''} \rangle \qquad (2.22)$$

where the vibronic wave functions are expressed by equation (2.21).

The electric dipole moment operator can be broken up into an electronic and a nuclear part:

$$M = M_e + M_N \quad . \tag{2.23}$$

If one substitutes equation (2.23) into equation (2.22) and simplifies, see reference (24), then equation (2.22) reduces to:

$$R_{e'v'e''v''} = R_{e'e''} < \psi_{v'} \mid \psi_{v''} > \tag{2.24}$$

where $R_{e'e''}$ is considered to vary only slightly with Q since the electronic wave function ψ_e contains both electronic and nuclear coordinates. The condition for $R_{e'e''}$ to be non-zero has already been given. Thus for C_6H_5NC the allowed electronic transitions from the ground singlet state A_1 are to excited singlet states of A_1, B_1, and B_2 symmetry. There are in addition selection rules for the integral $< \psi_{v'} \mid \psi_{v''} >$. This integral is non-zero only if the direct product representation $\Gamma(\psi_{v'}) \times \Gamma(\psi_{v''})$ is totally symmetric. Therefore in an allowed electronic transition, the lowest vibrational levels ($V_1 = V_2 = \ldots = 0$) of the two electronic states are always able to combine to give the origin (0-0) band. For a totally symmetric vibration the changes that can occur in the vibrational quantum number V_S are:

$$\Delta V_S = V_{S'} - V_{S''} = 0, \pm 1, \pm 2, \pm 3, \ldots \tag{2.25}$$

Thus levels which represent any number of quanta of a totally symmetric vibration excited in either electronic state can combine spectroscopically, while the only changes permitted for the vibrational quantum numbers of non-totally symmetric vibrations are:

$$\Delta V_a = V_{a'} - V_{a''} = 0, \pm 2, \pm 4, \ldots \tag{2.26}$$

2.11 Vibronic Interactions

The electronic wave functions are dependent on the nuclear coordinates Q and consequently vibronic interactions occur for polyatomic molecules having only non-degenerate electronic states. When totally or non-totally symmetric vibrations are excited, vibronic interactions mix zeroth order electronic states $\psi_e(q, Q)$. This type of interaction is known as the Herzberg-Teller effect[25]. The extent of interaction is important because a large degree of interaction might make allowed transitions which previously would have caused $R_{e'e''}$ to be zero, that is that were previously forbidden. The Herzberg-Teller theory treats the nuclear motion as a perturbation in the electronic equation:

$$H_e (q, Q)\ \psi_e (q, Q) = E_e (Q)\ \psi_e (q, Q) \tag{2.27}$$

because in a higher approximation, the electronic Hamiltonian, H_e and especially the terms V_{en} vary as the nuclear coorindates vary.

While it is possible, in principle, for two electronic states of any species to perturb each other if suitable vibrations are excited, this perturbation will be very weak unless the species of the two electronic states do not differ by more than the species of one of the normal vibrations[24]. This may be expressed as:

$$\Gamma(\psi_a) \times \Gamma(\psi_b) = \Gamma(Q_\alpha) \qquad (2.28)$$

where ψ_a is the perturbing electronic state, ψ_b is the perturbed electronic state and Q_α is the normal coordinate representative of the vibration causing the perturbation.

A forbidden component has been found in the spectra of certain aromatic molecules such as ethynylbenzene and in this study for phenyl isocyanide. A treatment of the Herzberg-Teller effect can be found in reference (17).

2.12. Franck-Condon Principle

The shape of an absorption or emission band due to a single electronic transition will be influenced by the superposition of vibrational transitions on this electronic transition and the relative intensities of the vibrational subbands will be governed by the Franck-Condon principle. This principle is based upon the assumption that during an electronic transition the nuclei do not change their positions or their momenta.

Thus the most probable vibrational component of an electronic transition should therefore be the one which involves no change in the nuclear configuration. This is reasonable to expect since an electronic transition is much faster (10^{-15} sec) than the nuclear motion (10^{-12} sec).

In the approximation of slowly varying electronic transition moment and separability of electronic, rotational and vibrational parts of the total wave function, the relative intensities of the vibrational components of an electronic absorption or emission band will depend largely on the square of the overlap integral between the vibrational wave functions of the ground and excited state. This overlap integral is known as the Franck-Condon overlap integral or Franck-Condon factor. This is the integral in equation (2.24).

In reference to Figure 2.3, the most probable transition will, according to the Franck-Condon principle, be a vertically upward (absorption) or downward (emission) as shown in the potential energy diagram.

The oscillator corresponding to a real molecule is never at rest and in the V = 0 vibrational level a probability distribution describes the internuclear separation. What this means is that the transitions may originate from the V = 0 level over a certain range of r values. This is why more than one band originating from V = 0 is observed.

If upon excitation, the molecular geometry of the excited state is nearly the same as the ground state then the most probable transition and most intense band in the emission spectrum will be the (0-0) band with the

Figure 2.3

Franck-Condon potential curves for the ground and lowest excited states (a,c) and the resulting expected emission progression (b,d).

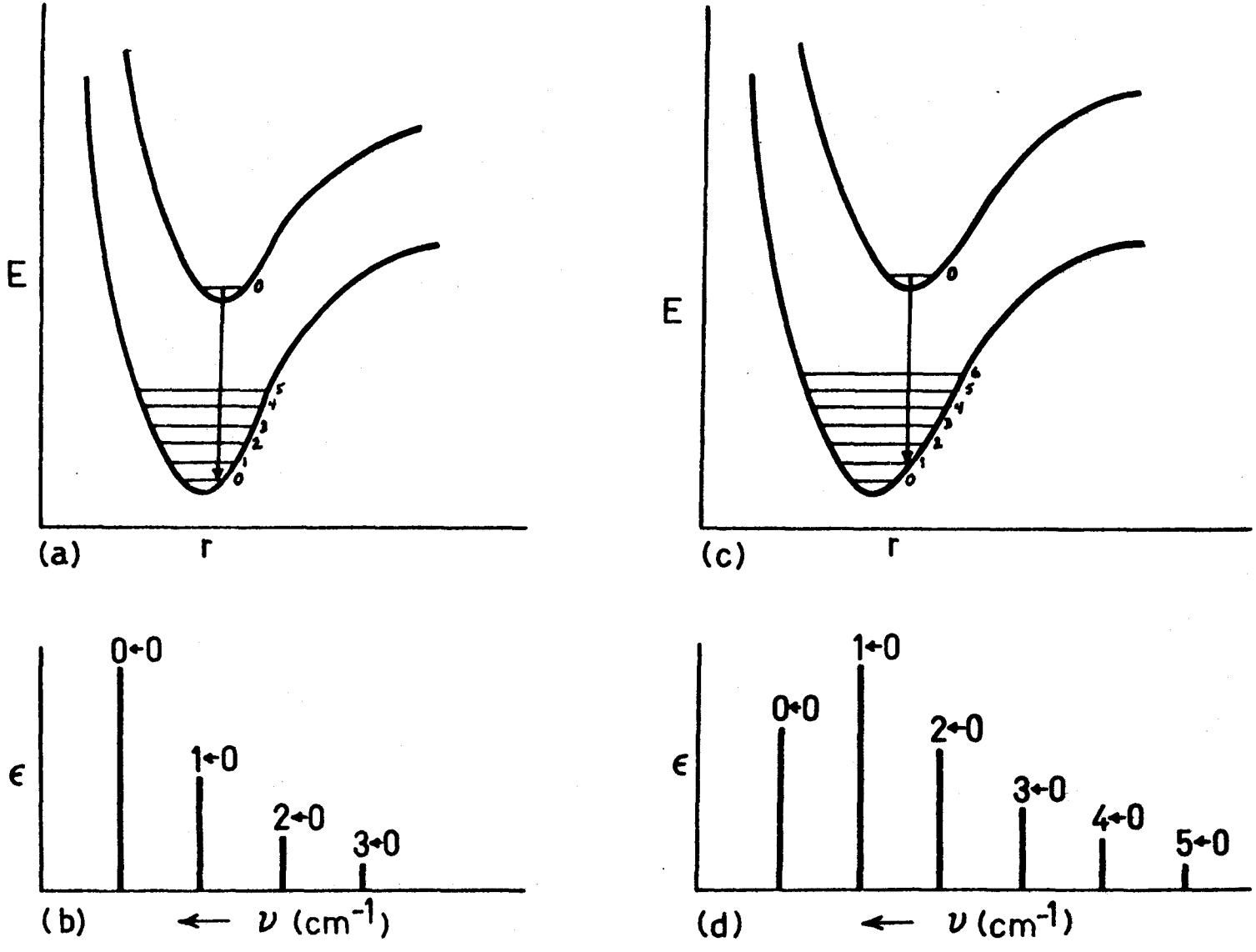

Figure 2.3 Franck-Condon potential curves for the ground and lowest excited states (a,c) and the resulting expected emission progression (b,d).

intensity of the other bands falling off quite rapidly as shown in Figure 2.3. However, if the excited state geometry is significantly different from that of the ground state, in which case the minimum of the excited state potential energy curve would be displaced with respect to that of the ground state, then one would expect to see a longer progression, with the (0-0) no longer the most intense band, since the V = 0 level of the excited state now overlaps with more levels of the ground state. Thus, the most prominent vibrational progression provides useful information about a change in molecular geometry upon excitation.

2.13 Phosphorescence and Fluorescence

A molecule having absorbed radiation has several paths to lose this energy and become stable again. Some of these mechanisms are radiative such as fluorescence and phosphorescence and others are radiationless. The formation of photochemical products is also possible. Figure 2.4, known as a Jablonski diagram, shows the possible mechanisms for an excited state molecule to lose its energy when it is in a condensed medium. The radiative processes are represented by a solid vertical arrow for transitions between states of the same multiplicity and a dashed vertical arrow for transitions between states of different multiplicity. The non-radiative transitions are depicted by a vertical wavy arrow for vibrational relaxation, a horizontal dashed arrow for intersystem crossing, and a solid horizontal arrow for internal conversion.

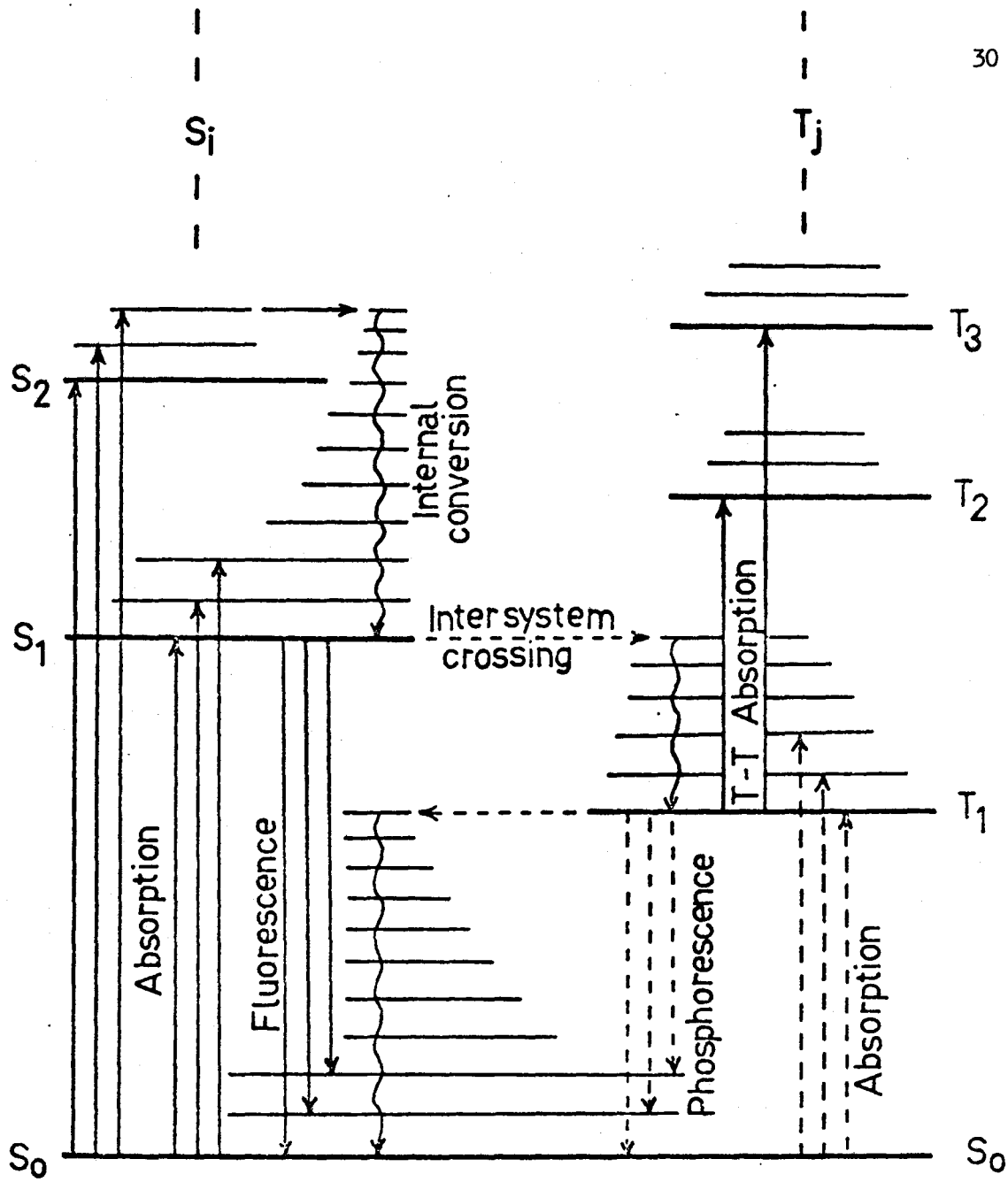

Figure 2.4 Schematic energy levels with the possible absorption transitions and different types of mechanisms for intramolecular loss of energy.

The process $S_o \rightarrow S_i$ puts a molecule into an excited singlet state. After having been excited to S_i, i.e., (S_2), the molecule will undergo internal conversion which is defined as a radiationless passage between two different electronic states of the same spin multiplicity[26]. The excess vibrational energy of S_1 is now removed by a process called vibrational relaxation until a thermally equilibrated (relative to the minimum of the S_1 potential energy surface) ensemble of S_1 molecules is produced. This vibrational relaxation process is intermolecular, with energy being transferred to the medium while internal conversion is considered intramolecular.

The molecule is now in the vibrationless level of the first excited singlet state: There now are a number of possible processes which may occur.

1) Fluorescence, $S_1 \rightarrow S_0$, which is defined as an emission between two levels of the same multiplicity.
2) Internal conversion, $S_1 \rightsquigarrow S_0$, followed by vibrational relaxation.
3) Intersystem crossing $S_1 \rightsquigarrow T_1$ to the lowest triplet state.

Intersystem crossing is a radiationless passage from an electronic state in a singlet manifold to an electronic state in the triplet manifold or vice versa. Thus intersystem crossing from S_1 is the process for population of triplet states of organic molecules under ordinary conditions of illumination.

The great difference in $S_1 \rightsquigarrow T_1$ (10^4 - 10^{12} sec^{-1}) and $T_1 \rightsquigarrow S_0$ (10^{-1} - 10^5 sec^{-1}) intersystem crossing rates lies in the fact that the energy

gap $T_1 - S_0$ is usually greater than the $S_1 - T_1$ gap, and that T_j states may lie between S_1 and T_1 whereas none may be found between T_1 and S_0. Kasha[27] suggests that the probability of the process $S_1 \rightsquigarrow T_1$ increases as the energy gap between S_1 and T_1 decreases. Robinson[28,29,30] has proposed a theory which implies exceedingly high sensitivity of k_{ISC} ($T_1 \rightsquigarrow S_0$) to the energy gap $T_1 - S_0$. This extreme sensitivity to the energy gap is found in the vibrational overlap integrals, $\langle \psi'_v \mid \psi''_v \rangle$, of the two states between which energy is being non-radiatively transferred. This sensitivity should be common to both intersystem crossing and internal conversion and should not be influenced by the spin reorientation process.

With the molecule now in the triplet state, the following processes may occur:

1) Vibrational relaxation to the vibrationless level of the lowest triplet state, followed by
2) Phosphorescence to the ground singlet state. Phosphorescence is defined as the emission between two states of the same molecule which are of different spin multiplicity.
3) Intersystem crossing to the ground singlet state $T_1 \rightsquigarrow S_0$, followed by vibrational relaxation.

A look at Table 2.3 of the rate constants involved in the various processes of energy transfer shows quite a range of values. It is because of these differences in rate constants that phosphorescence and fluorescence emissions do occur. Although both the direct absorption $S_0 \rightarrow T_1$ and inter-

TABLE 2.3

Rate Constants for Radiative and Radiationless Processes

Process	Rate Constant (sec^{-1})
Absorption $S \rightarrow S_i$	$10^{15} - 10^{16}$
Internal conversion $S_2 \rightsquigarrow S_1$	$> 10^{12}$
Vibrational relaxation within S_1	$> 10^{12}$
Fluorescence $S_1 \rightarrow S_0$	$10^{6} - 10^{9}$
Internal conversion $S_1 \rightsquigarrow S_0$	$10^{6} - 10^{12}$
Vibrational relaxation within S_0	$> 10^{12}$
Intersystem crossing $S_1 \rightsquigarrow T_1$	$10^{4} - 10^{12}$
Vibrational relaxation within T_1	$> 10^{12}$
Phosphorescence $T_1 \rightarrow S_0$	$10^{-2} - 10^{4}$
Intersystem crossing $T_1 \rightsquigarrow S_0$	$10^{-1} - 10^{5}$

system crossing $S_1 \rightsquigarrow T_1$ are spin forbidden they are not equally probable. This is because the magnitude of spin-orbit coupling is inversely proportional to the energy differences between the triplet and singlet states concerned. Therefore, when the $T_1 - S_0$ energy differences, commonly of the order of 3000 - 9000 cm^{-1} are compared, the intersystem crossing probability ($S_1 \rightsquigarrow T_1$) should be greater than the direct transition from the ground singlet to the lowest triplet state. Although the $S_1 \rightsquigarrow T_1$ process is slower than the fluorescence process $S_1 \rightarrow S_0$ it is still fast enough to compete favorably with the fluorescence process and populate the triplet state.

It should be noted that emission whether by fluorescence or phosphorescence is usually from the first excited singlet and lowest triplet state, respectively, in accordance with Kasha's Rule[26].

2.14 Phosphorescence Lifetimes

After withdrawal of the exciting source the intensity of phosphorescence emission decays according to a first order rate equation, that is exponentially with time:

$$I = I_o e^{-t/\tau} \tag{2.29}$$

where I_o is some initial intensity at an arbitrary time zero, I is the intensity at some later time t, and τ is a constant. When the intensity has fallen to 1/e of its initial intensity I_o, the time t over which the decay is

measured will be equal to τ. This quantity τ is known as the mean decay time for the emission process or the mean lifetime of the excited state. The τ will be equal to τ_o, the intrinsic or natural lifetime, only if there are no deactivational processes, otherwise in terms of rate constants it is written as:

$$\tau = 1/\Sigma\, k_i \qquad (2.30)$$

where τ is the observed lifetime, $\Sigma\, k_i$ represents the sum of the phosphorescence rate constant k_{Ph} plus all rate constants related to deactivational processes. Phosphorescence lifetimes vary with temperature and solvent.

2.15 Properties of Polycrystalline Matrices and Glasses

It is sometimes possible in the gas phase to observe emission from the same vibronic level which had previously taken part in an absorption process. This is known as resonance fluorescence. However, in a matrix the level from which emission takes place is governed by Kasha's Rule, as was previously mentioned. This difference is shown in Figure 2.5a. For the type of matrices and glasses used in this work, i.e., organic solvents, the interactions between host molecules, between host lattice and guest species isolated in the host, and guest-guest interactions are weak[31]. Likewise for organic glasses, both the solvent-solvent and the solvent-solute interactions are weak. As a result of only weak interaction, the optical properties of the guest are usually characteristic of the free

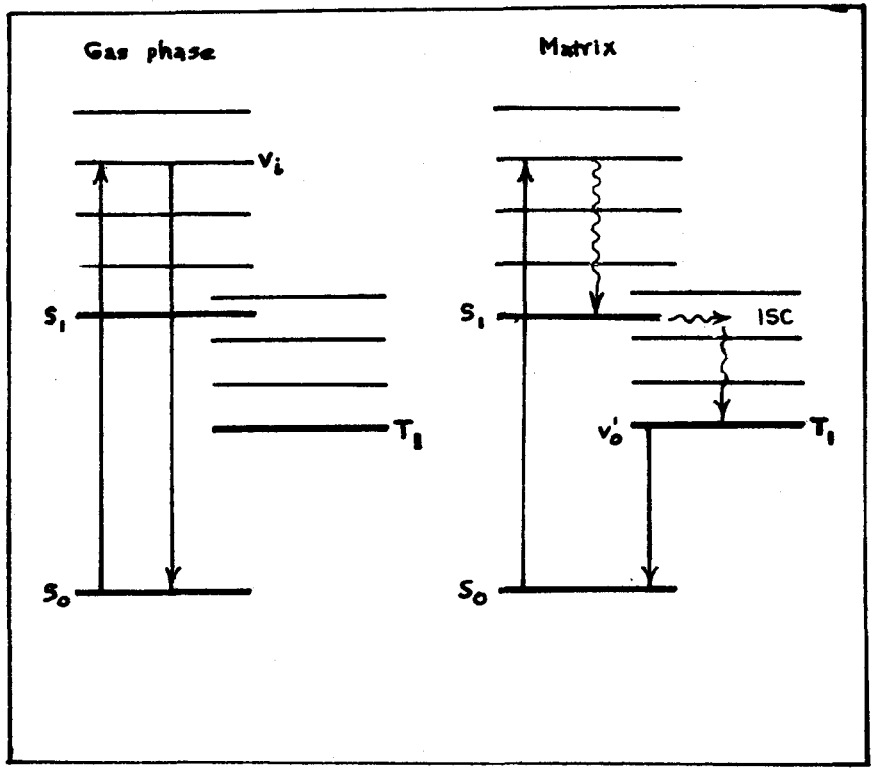

(a)

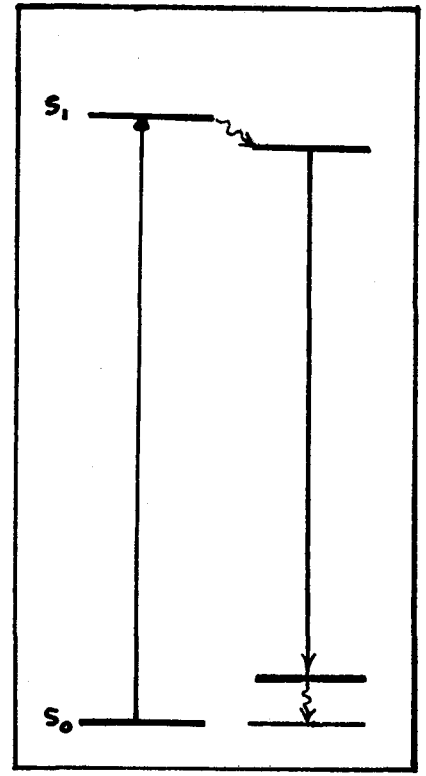

(b)

Figure 2.5a Comparison of gas phase and matrix emissions.
b Shift of (0,0) of absorption versus emission.

guest molecule, and host-guest interactions exert comparatively small distortions on the guest electron configuration. One does not have to worry about host absorption because in these matrices and glasses the lowest host energy level is high above the guest levels studied. In studies of guest molecules imbedded in rigid host matrices the ratio of host to guest molecules can be very large, and thus the guest species may be considered as an infinitely dilute cold gas.

The wavelengths of electronic and vibrational transitions of a guest isolated in a cold host are generally found to be shifted by less than 1% of the gas phase transition energy. Thus one does not generally see the (0-0), ($S_0 \rightarrow S_1$) absorption in the gas phase to coincide with the (0-0), ($S_1 \rightarrow S_0$) fluorescence emission of that molecule in a cold matrix. Figure 2.5b shows what happens.

In a cold matrix the guest molecule is surrounded by the host molecules unlike what is found in the gas phase. Now, upon absorption in the cold matrix the guest is in an unstable excited state configuration relative to the surrounding solvent molecules. The guest molecule will then attain a stable equilibrium before emitting. This configuration and therefore the level from which the emission occurs will be lower in energy. After emission the molecule finds itself in an unstable ground state with respect to the solvent and relaxes to the most stable configuration. Figure 2.5b shows one possibility, i.e., a red shift of the (0-0). However, depending on the magnitude of the interactions it is also possible to observe a blue shift.

It is possible to have multiple site emission in the matrices. For example, emission of the solute in two different crystalline environments of the solvent cyclohexane has been observed[32]. Cyclohexane has both a high temperature cubic form and a low temperature monoclinic form. The resulting emission showed a splitting of all the prominent bands. Emission of the solute in two different orientations is also possible[9].

When luminescence spectra are taken in certain organic solvents one observes what is known as the Shpol'skii effect. This refers to the fairly well resolved vibronic structure in the spectrum. In these solutions the dimensions of the solute molecule must approximate that of the solvent. One would expect to obtain a sharper spectrum when the molecule under study is caged or trapped in a rigid matrix because of the reduction of vibrational and rotational energy. The spectra tend to become diffuse in proportion to the degree of mis-fit of solute and solvent[33].

2.16 Polarization of Luminescence

The electric dipole transition integral contains the electric dipole moment operator M which is a vector, having components M_x, M_y and M_z. Therefore, one would expect an oriented molecule frozen in a glass to be anisotropic to polarized electromagnetic radiation.

In the method of photoselection described by Albrecht[34] molecules are randomly "frozen" in a glass and selectively excited with light

polarized in a particular plane. Therefore only molecules having absorption transition moments parallel to the electric vector of the exciting light will be excited preferentially. Molecules with other orientations will contribute less to the total intensity of the transition.

The degree of polarization is defined as:

$$\rho = \frac{I_{VV} - I_{VH}}{I_{VV} + I_{VH}} = \frac{(3 \cos^2 \alpha) - 1}{(\cos^2 \alpha) + 3} \qquad (2.31)$$

where I_{VH} is the intensity of emission after the molecule has been excited with vertically polarized light and the emission passed through a polarizer letting through only horizontally polarized light; I_{VV} is the intensity of emission when the exciting polarizer is the same as above but the analyzing polarizer is letting through vertically polarized light; α is the angle between the emission and absorption transition moments.

Under ideal conditions parallel electric dipoles give a maximum value of + 1/2 for the polarization and perpendicular electric dipoles give a maximum value of - 1/3.

2.17 Assignment of the Lowest Triplet State

In phenyl isocyanide the π-π^* transitions are in-plane polarized, which under C_{2V} symmetry corresponds to $A_1 \leftrightarrow B_2$ ($S_0 \rightarrow S_1$) and $A_1 \leftrightarrow A_1$ ($S_0 \rightarrow S_2$). Since the degree of polarization is dependent upon the direction of the electric dipole moment of the absorbing and emitting

states, this quantity will be different when exciting into the (0-0) of S_1 and S_2. Thus a $^1A_1 \rightarrow {}^1B_2$ absorption and $^1B_2 \rightarrow {}^1A_1$ fluorescence should produce a positive degree of polarization since the absorption and emission transition moments (y) are parallel. However, $^1A_1 \rightarrow {}^1A_1$ absorption followed by $^1B_2 \rightarrow {}^1A_1$ emission have perpendicular transition moments since $^1A_1 \rightarrow {}^1A_1$ has a transition moment in the (z) direction. Therefore one obtains a negative degree of polarization for this combination of absorption and emission.

The symmetry of the lowest triplet state may be assigned by determining the polarization of the (0-0) phosphorescence band. This is done by exciting into the (0 ,0) region of the (S_0-S_1) band and then the (0,0) region of the (S_0-S_2) band while monitoring the phosphorescence (0-0) band.

A transition whether radiative or nonradiative between states of different multiplicity is spin forbidden. This forbiddenness is relaxed by an interaction between the magnetic dipole moment generated by the intrinsic spin of the electron and the magnetic dipole moment generated by the orbital motion of the electron. This interaction is known as spin-orbit coupling. The result of this interaction will be to introduce or mix some singlet character into the triplet state and some triplet character into the singlet state.

The wave function of the lowest triplet state, T', perturbed by admixture with singlet states, s^k, is expressed as:

$$\psi(T') = \psi(t') + \sum_k \frac{\langle t'|H_{SO}|s^k\rangle}{E(t') - E(s^k)} \psi(s^k) \qquad (2.32)$$

and the wavefunction of the ground singlet state, S^o, perturbed by triplet states, t^k, is expressed as:

$$\psi(S^o) = \psi(s^o) + \sum_k \frac{< s^o|H_{SO}|t^k >}{E(s^o) - E(t^k)} \psi(t^k) \qquad (2.33)$$

where $\psi(t')$ and $\psi(s^o)$ are the unperturbed lowest triplet and singlet states respectively and where H_{SO} is the spin-orbit Hamiltonian operator which has the form:

$$H_{SO} = - \left[\frac{h^2}{(2mc)^2} \right] (\nabla V X p) \cdot S \, . \qquad (2.34)$$

where h and c are Planck's constant and the speed of light; m is the mass of an electron; ∇V is the gradient of the potential energy.

McClure[35] has shown that the orbital part of H_{SO} transforms as axial rotations R_x, R_y, R_z.

The transition moment of the singlet-triplet transition is:

$$M = < S^o|er|T' > = \sum_k < s^o|er| \frac{<t'|H_{SO}|s^k>}{E(t') - E(s^k)} s^k > + \sum_k < t'|er| \frac{<S^o|H_{SO}|t^k>}{E(S^o) - E(t^k)} t^k > \qquad (2.35)$$

In order for the transition moment to be non-zero, at least one of the "k" mixing coefficients:

$$\frac{\langle t'|H_{SO}|s^k\rangle}{E(t') - E(s^k)} \qquad \text{and} \qquad \frac{\langle s^o|H_{SO}|t^k\rangle}{E(s^o) - E(t^k)}$$

must be non-zero.

The degree of mixing is related to several factors:

(a) The potential field of the nucleus.

(b) The magnitude of spin-orbit coupling is inversely proportional to the energetic separation of the triplet and the perturbing or mixing singlet.

If the lowest triplet state is of $^3A_1$ orbital symmetry and H_{SO} transforms as axial rotations, R_x, R_y and R_z then by direct product calculations, it is found that the perturbing triplet states to s^o may be $^3A_2$, $^3B_1$ and $^3B_2$ since the direct product of the triplet state symmetry, the spin-orbit Hamiltonian H_{SO} and possible perturbing singlets must be totally symmetric. The perturbing singlet states to t' can be $^1A_2$, $^1B_1$ and $^1B_2$. However, the transition moment for a singlet-triplet transition, equation (2.35) is also influenced by the integrals $\langle s^o|er|s^k\rangle$ and $\langle t'|er|t^k\rangle$ and it is the direction of polarization of the transitions $s^o \rightarrow s^k$ and $t' \rightarrow t^k$ which determine the polarization of the phosphorescence. Thus s^k may be $^1B_1$ and $^1B_2$ while t^k may be $^3B_1$ and $^3B_2$. The polarizations of $^1A_1 <-> {}^1B_1$ and $^1A_1 <-> {}^1B_2$ are out-of-plane (x) and short axis in-plane (y) respectively as are the $^3A_1 <-> {}^3B_1$ and $^3A_1 <-> {}^3B_2$ transitions.

For a $^3B_2$ orbital symmetry for the lowest triplet state, different perturbing states and polarizations are expected; these are shown in Table 2.4.

Table 2.4 shows that for both choices of the lowest triplet state symmetry, $^3A_1$ and $^3B_2$, an out-of-plane polarization (x) contribution to the polarization of the (0-0) phosphorescence band is possible. However, they differ in that for $^3A_1$, a short axis in-plane (y) contribution is expected while for $^3B_2$, there can be a long axis in-plane (z) contribution.

Thus one obtains the lowest triplet state symmetry by determining the degree of polarization of the (0-0) phosphorescence band exciting in $S_1(y)$ and $S_2(z)$ while monitoring the (0-0) of phosphorescence because for a $^3A_1$ lowest triplet, the polarization ratio would be more positive for a $(S_0 - S_1)$ (y) excitation while for a $^3B_2$ assignment, the ratio would be more positive for the $(S_0 - S_2)$ (z) excitation.

TABLE 2.4

Spin-Orbital Mixing of Singlet and Triplet States

Lowest Triplet State t^k (orbital symmetry)	H_{so} (transform as R's)	Possible Perturbing Singlet States s^k to the Lowest Triplet State and Polarization of $s^k \rightarrow s^o$	Possible Perturbing Triplet States t^k to the Ground State and Polarization of $t^k \rightarrow t^l$
$^3B_2$	A_2	$^1B_1(x)$	$^3A_2(x)$
	B_1	$^1A_2$ (forbidden)	$^3B_1$ (forbidden)
	B_2	$^1A_1$ (z)	$^3B_2$ (z)
$^3A_1$	A_2	$^1A_2$ (forbidden)	$^3A_2$ (forbidden)
	B_1	$^1B_1$ (x)	$^3B_1$ (x)
	B_2	$^1B_2$ (y)	$^3B_2$ (y)

CHAPTER III

EXPERIMENTAL

3.1 Chemicals

C_6H_5NC was prepared according to reference (36) and by the method of Ugi and Meyr[37].

Formanilide C_6H_5NHCHO, the required starting material for the method of Ugi and Meyr was synthesized from aniline and formic acid in toluene. Colorless vile-smelling liquid phenyl isocyanide tended to turn green immediately upon preparation; after a final distillation under vacuum, the product was stored at dry ice temperature until use.

C_6D_5NC was prepared in 50% yield from ring deuterated aniline by the same method[37,38], the formanilide not being isolated. Ring deuterated aniline was made by the oxidation of perdeuterotoluene, a Stohler Isotope Chemicals product, with potassium permanganate, followed by the treatment of the resulting ring deuterated benzoic acid with sodium azide and sulfuric acid. The steps taken in the C_6D_5NC preparation are shown below:

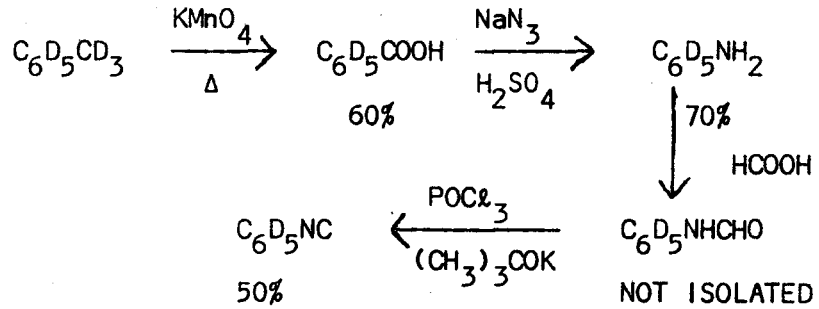

No evidence of the isomer C_6H_5CN was found in the infrared. The C_6H_5NC infrared spectrum was in good agreement with that earlier published[15]. Proton NMR did not show any presence of non-aromatic proton impurities. Proton NMR of the C_6D_5NC showed the presence of aromatic and non-aromatic at levels of approximately 1%.

3.2 Solvents

The solvents used for the luminescence work were: Methylcyclohexane, cyclohexane, spectroquality products of Matheson, Coleman and Bell were used without further purification, 3-methylpentane - a pure grade product of Phillip 66, was used after shaking in Linde 10X molecular sieve; 95% ethanol - grade unknown but showed no luminescence under experimental conditions used.

3.3 Apparatus

Infrared spectra of the C_6H_5NC and C_6D_5NC liquids were recorded on a Perkin Elmer Model 521 Spectrophotometer. KBr windows were used in both the sample and reference beams with path lengths of 0.025 to 0.100 mm. Polystyrene was used for calibration purposes. Accuracy of the sharp intense bands is estimated to be $\pm$ 1 cm^{-1} and ranges from $\pm$ 2 to $\pm$ 5 cm^{-1} for less resolved broad or weak bands.

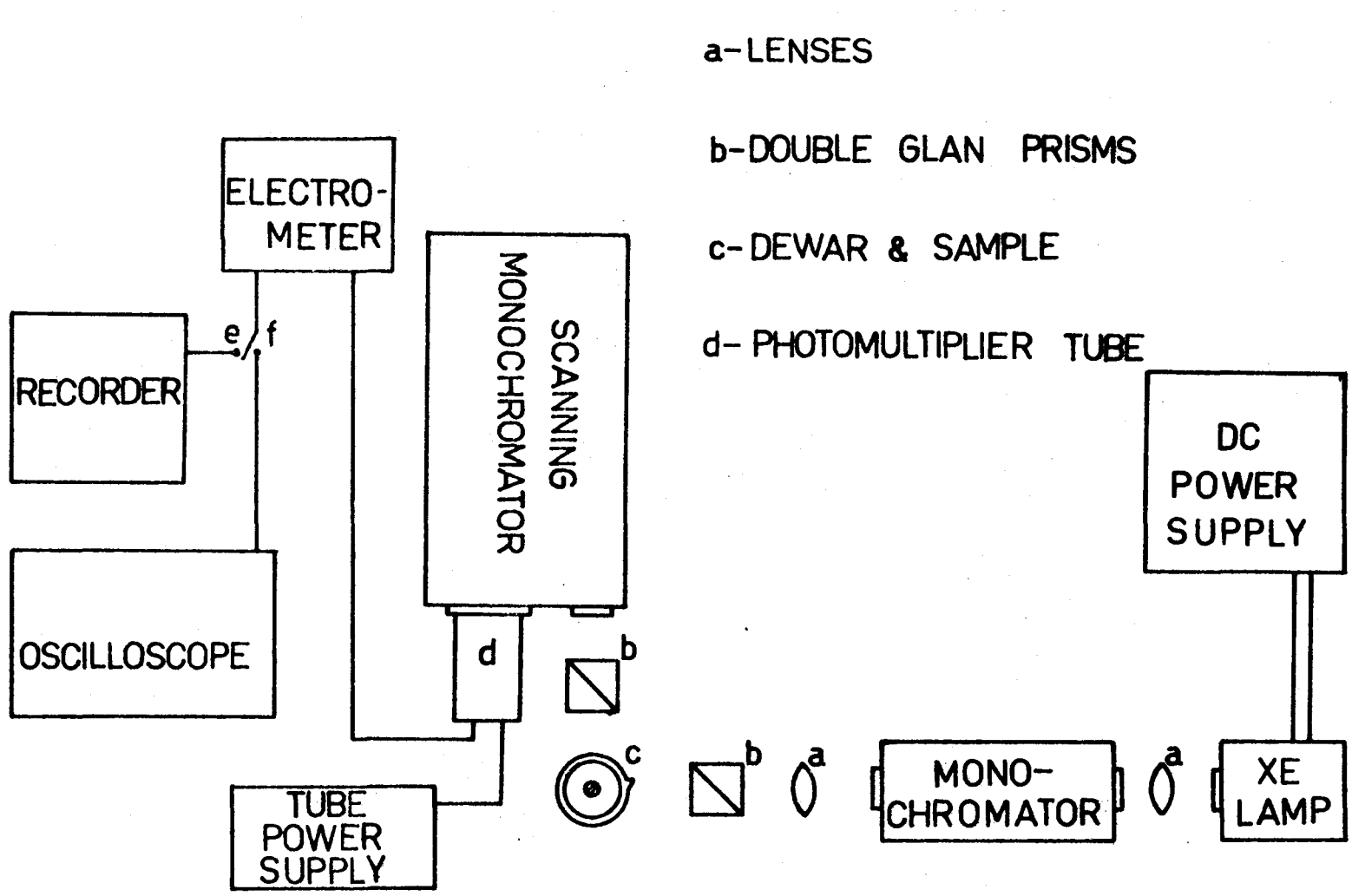

FIG. 3.1 APPARATUS FOR EMISSION EXPERIMENTS — BLOCK DIAGRAM

Raman spectra were obtained from liquid samples in sealed pyrex capillary tubes, either at room temperature or at -35°C. The excitation sources used were: the red 6328 Å line from a Spectra Physics Model 125 helium-neon laser or the green 5145 Å line from a Spectra Physics Model 164 argon ion laser. The scattered radiation was detected by an ITT Model FW130 photomultiplier after passage through a Spex Model 1400 0.75-m Czerny Turner monochromator, then amplified and recorded.

Depolarization ratios were measured by placing a rotatable polarizer between the sample and the monochromator. The sharp bands have an estimated accuracy of $\pm$ 2 cm^{-1}.

The apparatus used for the luminescence spectra is shown schematically in Figure 3.1. The excitation sources were Osram 150 Watt Xenon lamp powered by a Bausch and Lomb power supply #33-86-20 or an Osram 450 Watt Xenon lamp powered by a DC regulated Universal lamp power supply, Model #C-72-50, from Oriel Optics Corporation. The exciting light was then passed through a Jarrell-Ash 0.25 meter pathlength Ebert monochromator provided with a 2360 grooves/mm, 300 nm blazed grating.

The monochromated light was focused by means of a quartz lens onto the sample under study in a 11 mm O.D. quartz tube immersed in a partially silvered quartz dewar containing boiling liquid nitrogen.

The emitted radiation was passed through a 0.5 meter pathlength Jarrell-Ash scanning monochromator with a 1180 grooves/mm grating blazed at 400 nm, which was perpendicular to the exciting light. The emitted radiation was then detected by a RCA Type 8575 photomultiplier powered by a Power Design, Model HV 1544 power supply. The signal from the photomultiplier was treated in one of two ways before being fed into a Varian

G2000 chart recorder:

1. amplification by a Keithley Model 610C electrometer,
2. amplification by an Ortec Model 454 Timing Filter Amplifier, used in conjunction with an Ortec photon counting system consisting of a Model 421 Integral Discriminator, a Model 441 Ratemeter, and a 9201 Photomultiplier Base.

Phosphorescence lifetime measurements were obtained by feeding the signal from the electrometer into a Hewlett-Packard 132A Dual Beam Oscilloscope. The decay of the phosphorescence $(0,\nu_5)$ or $(0, 2\nu_5)$ band after the exciting light was mechanically shuttered, was photographed by means of a Hewlett-Packard Model 196B Oscilloscope camera. Concentrations of samples ranged from 10^{-3} - 10^{-4} M.

Polarization measurements of the emission were obtained by placing a UV polarizing Glan prism between the exciting monochromator and the sample and between the sample and the analysing monochromator. To minimize the "instrumental favoring" the following procedure was used: the exciting polarizer was set to pass only vertical electric vector light (V) and the intensity of emission was recorded for the horizontal (H) and vertical (V) position of the analysing polarizer. This gives the uncorrected polarization ratio, I_{VV}/I_{VH}. To obtain the correction factor, I_{HH}/I_{HV} one positions the exciting polarizer to pass only horizontal electric vector light (H) and the intensity of emission is again recorded for the horizontal and vertical position of the analysing polarizer. The product $I_{VV}.I_{HH}/I_{VH}.I_{HV}$

represents the corrected polarization ratio, N, from which is calculated the degree of polarization, ρ:

$$\rho = N-1/N+1 \qquad (3.1)$$

The solvents for polarization measurements were a 75% to 25% by volume mixture of 3-methylpentane to methylcyclohexane and an 80% to 20% by volume mixture of methylcyclohexane to 3-methylpentane. Samples were frozen for 2 hours prior to the measurements.

3.4 Cooling Methods

There were two main methods employed to cool the solutions used to obtain luminescence spectra:

1. The solution was rapidly immersed in a dewar of boiling liquid nitrogen, thus forming a glass. The solution was lifted out of the nitrogen and allowed to warm up until a small portion crystallized. It was then placed slightly above the level of the nitrogen until a new region crystallized, after which it was lowered progressively as a newer region crystallized until all the solution formed a polycrystalline mass.
2. The solution was placed slightly above the level of boiling liquid nitrogen in the dewar. After a portion had crystallized it was

lowered until a new region crystallized and this process was repeated until all the solution crystallized.

Luminescence spectra were taken of 10^{-3} - 10^{-4} M solutions. Estimated accuracy of the luminescence spectra is $\pm$ 1 Å. Calibration was performed with Xe and Hg lines.

Ultraviolet absorption spectra of both phenyl and perdeutero-phenyl isocyanide were recorded on a Cary 14 double beam recording spectrophotometer.

The intensity of infrared, Raman, and luminescence spectra were not corrected for monochromator-photomultiplier response.

CHAPTER IV

INFRARED AND RAMAN ANALYSIS

An analysis of the infrared and Raman spectra is now presented. A schematic diagram of the approximate descriptions for some normal modes of monosubstituted benzenes is shown in Figure 4.1. These descriptions by Randle and Whiffen[39] were made by treating the substituent group as a single unit X.

The assignments of the infrared and Raman spectra are found in Table 4.3. The ground state fundamental frequencies for C_6H_5NC and C_6D_5NC are given in Table 4.4. A detailed account of the abbreviations used for the description of the fundamentals is presented in Table 4.1. Also listed in Table 4.2 are the expected frequency ranges for monosubstituted perprotonated benzenes and perdeuterated monosubstituted benzenes. Infrared and Raman spectra are shown in Figures 4.2 and 4.3.

Phenyl isocyanide has 33 normal modes of vibration. Assuming C_{2V} symmetry in the ground state these give rise to $12a_1$, $3a_2$, $7b_1$, and $11b_2$ symmetry species. Of these, all except the $3a_2$ are theoretically infrared active.

However, the $3a_2$ modes do appear in the I.R. spectrum of C_6H_5NC. One of these ν_{14}, (g) in Whiffen's notation, appears as a band of medium intensity in C_6H_5NC. An a_2 band of medium intensity is also observed in the liquid infrared of toluene[40]. The other a_2 modes

appear weakly. In C_6D_5NC only one of the a_2 species is seen, ν_{14} (g). These three a_2 modes are also seen in the liquid infrared of C_6H_5CCH[4] and C_6H_5CN[7]. It has been suggested that such infrared inactive bands do occur in many cases because of perturbations by the liquid environment[41,42]; however two of the modes ν_{13} (h) and ν_{14} (g) are even seen in the vapor phase spectra of C_6D_5CN[8].

In the infrared spectrum of C_6H_5NC all of the fundamentals appear except for ν_{22} (y) which is below the transmission limits of the KBr windows. This fundamental is detected in the Raman.

In the infrared of C_6D_5NC all of the fundamentals except ν_{13} (h), ν_{15} (w), ν_{16} (j), ν_{21}, ν_{22} (y) and ν_{33} (u) are seen. The frequencies for ν_{13} and ν_{15} have been estimated from combination bands. The fundamental ν_{16} is observed in the Raman. The vibrations ν_{21} and ν_{33} which are considered accidently degenerate are below the transmission limits of KBr as is ν_{22}, but appear in the Raman. Band ν_{16} (j) for C_6D_5NC is only seen in the Raman. In the infrared it is possible that it is hidden under the medium intensity band ν_{29} (c).

In the Raman spectra, not nearly as many fundamentals were seen as in the infrared. The most prominent bands were of a_1 symmetry. A few overtone and combination bands were also detected. Although the a_2 modes are Raman active they are not seen, as is the case with C_6H_5CCH. Only one is seen in the Raman for C_6H_5CN. The Raman spectra with its relatively few bands and the prominence of the totally symmetric a_1 modes, along with the depolarization ratios obtained, make its analysis much easier than that of the more complicated infrared spectra.

The analysis of the infrared and subsequent assignment of the 33 normal modes of phenyl isocyanides was aided by the fact that vibrational analyses of some monosubstituted benzenes have been carried out in the past[4,43,44,45] and it was found that twenty-four vibrations of these molecules are essentially insensitive to the nature of the substituent. Table 4.2 based on the study of a number of monosubstituted benzenes and ring deuterated monosubstituted benzenes shows the expected frequency range for the vibrations. Also two molecules isoelectronic with C_6H_5NC, namely C_6H_5CCH and C_6H_5CN have been completely analyzed and thus C_6H_5NC would be expected to have similar frequencies, especially for vibrations which are essentially mass dependent. Another aid to the vibrational analysis are the Raman depolarization ratios which help distinguish totally symmetric fundamentals from nontotally symmetric ones. The validity of a_1 mode assignments are further enhanced by a calculation of the Teller-Redlich product ratio. Assignments of fundamentals have also been made by comparing intensities of the bands in the C_6H_5NC and C_6D_5NC spectra. A distinction between fundamental bands and overtone or combination bands was in general made by noting their intensities. The vibrations of phenyl isocyanide are governed by the two large masses of the ring and the substituent. Thus the analysis is aided by the expected shifts of ring vibrations in the spectrum of C_6D_5NC. Also of help to the analysis are the luminescence spectra of C_6H_5NC and C_6D_5NC[46].

Although assignments are listed for the combination bands they are certainly not the only possible choices. Those listed are based on the intensities of the combining fundamentals.

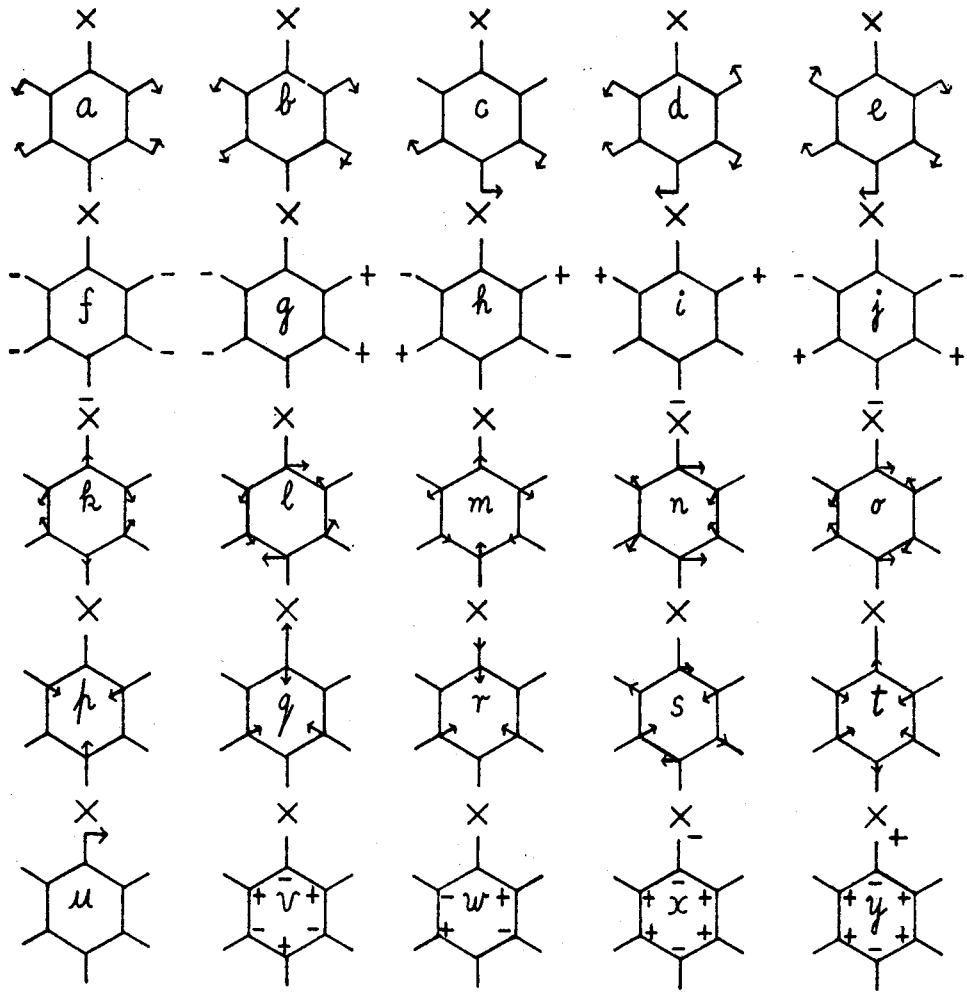

Figure 4.1 Some schematic vibrational modes of monosubstituted benzenes.

TABLE 4.I

Descriptions of the Benzene Ring Vibrations and Those of the Substituent, -NC

Abbreviation	Description
ν C-H	C-H stretching
β C-H	C-H in-plane deformation
γ C-H	C-H out-of-plane deformation
ν C-C	C-C stretching
α C-C-C	ring in-plane deformation
ϕ C-C	ring out-of-plane deformation
Ring	ring breathing
ν C-NC	C-N stretching between benzene ring and isocyanide group
β C-NC	C-N in-plane deformation between benzene ring and isocyanide group
γ C-NC	C-N out-of-plane deformation between benzene ring and isocyanide group
ν N≡C	N≡C stretching
β N≡C	N≡C in-plane deformation
γ N≡C	N≡C out-of-plane deformation
X-sens	substituent X sensitive vibrations in which X moves with appreciable amplitude and thus the frequencies are sensitive to the mass of X

TABLE 4.2

Range of Frequencies of Fundamentals of Monosubstituted Benzenes (cm^{-1})

Designation[a]	C_6H_5X[b]	C_6H_5NC	C_6D_5X[d]	C_6D_5NC
ν_1	3010-3120	3089	2260-2305	2303
ν_2		3071		2283
ν_3		3046		2262
ν_4	2120[c]	2125		2123
k ν_5	1575-1614	1595	1535-1580	1565
m ν_6	1470-1515	1485	1320-1390	1368
q ν_7	1100-1280	1185	990-1230	1123
a ν_8	1170-1181	1163	860- 880	863
b ν_9	1019-1032	1026	795- 820	826
p ν_{10}	990-1010	998	950- 965	959
r ν_{11}	730- 830	762	620- 750	720
t ν_{12}	300- 530	469	260- 530	456
h ν_{13}	952- 975	967	760- 795	767[e]
g ν_{14}	824- 847	840	655- 695	696
w ν_{15}	$\approx$ 400	418	350- 380	370[e]
j ν_{16}	973- 985	989	810- 830	847
i ν_{17}	882- 938	914	735- 770	763
f ν_{18}	728- 797	753	605- 655	628
v ν_{19}	680- 700	680	510- 570	550

Table 4.2 (contd)

Designation[a]		C_6H_5X[b]	C_6H_5NC	C_6D_5X[d]	C_6D_5NC
x	ν_{20}	430- 560	512	350- 490	452
	ν_{21}		325		311
y	ν_{22}	140- 250	162	150- 230	160
	ν_{23}	3010-3120	3105	2260-2305	2283
	ν_{24}		3065		2262
l	ν_{25}	1562-1597	1587	1535-1580	1554
n	ν_{26}	1440-1470	1454	1305-1330	1334
o	ν_{27}	1300-1350	1328	1260-1295	1283
e	ν_{28}	1253-1331	1288	1000-1050	1036
c	ν_{29}	1150-1160	1157	830- 845	842
d	ν_{30}	1065-1082	1070	785- 835	817
s	ν_{31}	605- 630	613	585- 605	595
	ν_{32}		478		471
u	ν_{33}	200- 410	325	200- 390	311

a. The first column under this heading correlates the vibrational modes of the phenyl isocyanides with the labelling of the vibrational modes of monosubstituted benzenes by Whiffen (43). The second column is Herzberg's notation as applied to the phenyl isocyanides.

Table 4.2 (contd)

b. All the expected values are taken from reference (47) except ν_4.
c. Value taken from (15).
d. Values taken from (63).
e. Estimated value.

Figure 4.2

Infrared spectra of liquid phenyl isocyanide and perdeuterophenyl isocyanide

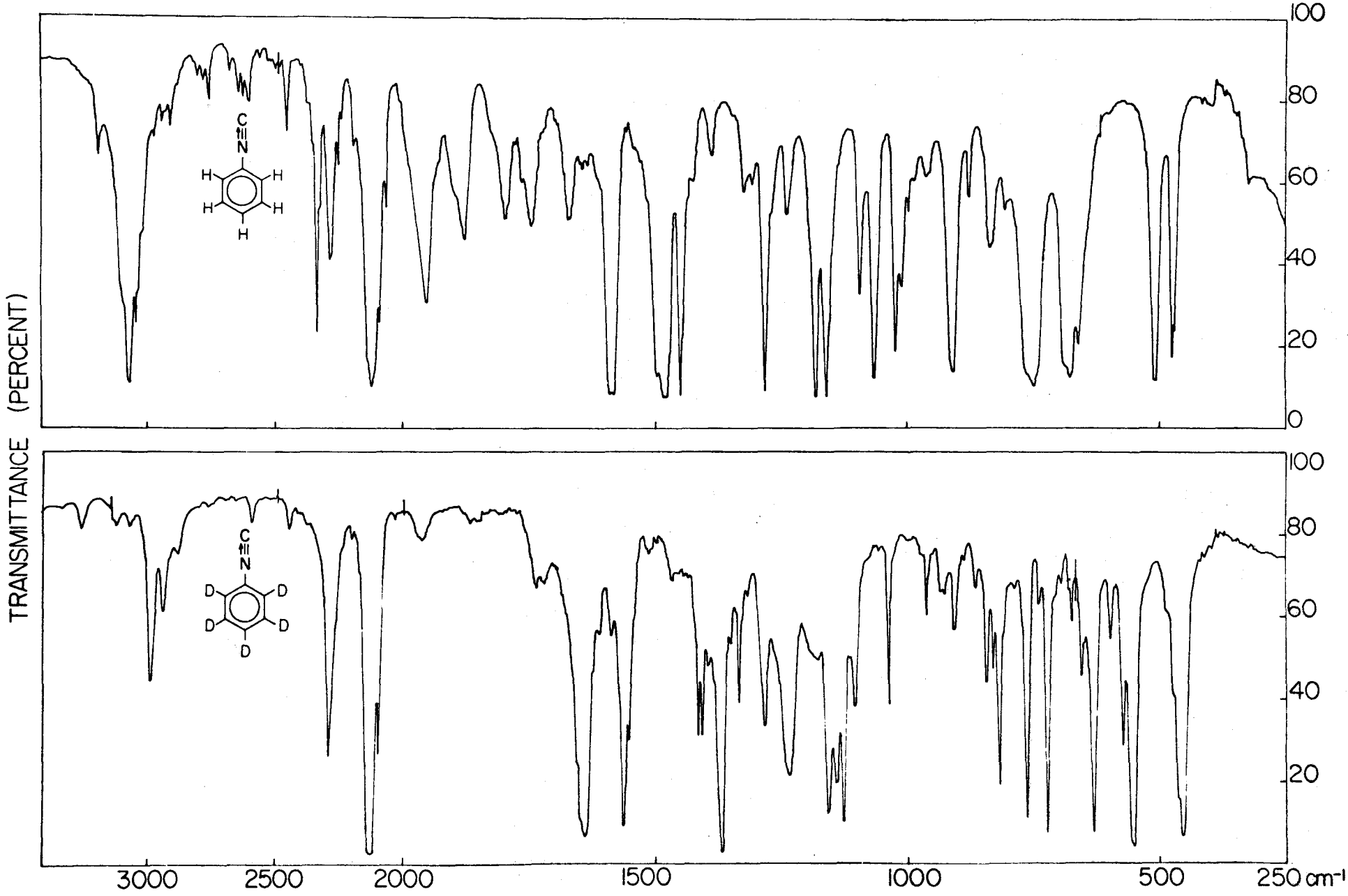
TRANSMITTANCE (PERCENT)
100
80
60
40
20
0
C≡N
H
H
H
H
H
100
80
60
40
20
C≡N
D
D
D
D
D
3000
2500
2000
1500
1000
500
250 cm-1

Figure 4.3

Raman spectra of liquid phenyl isocyanide and perdeuterophenyl isocyanide

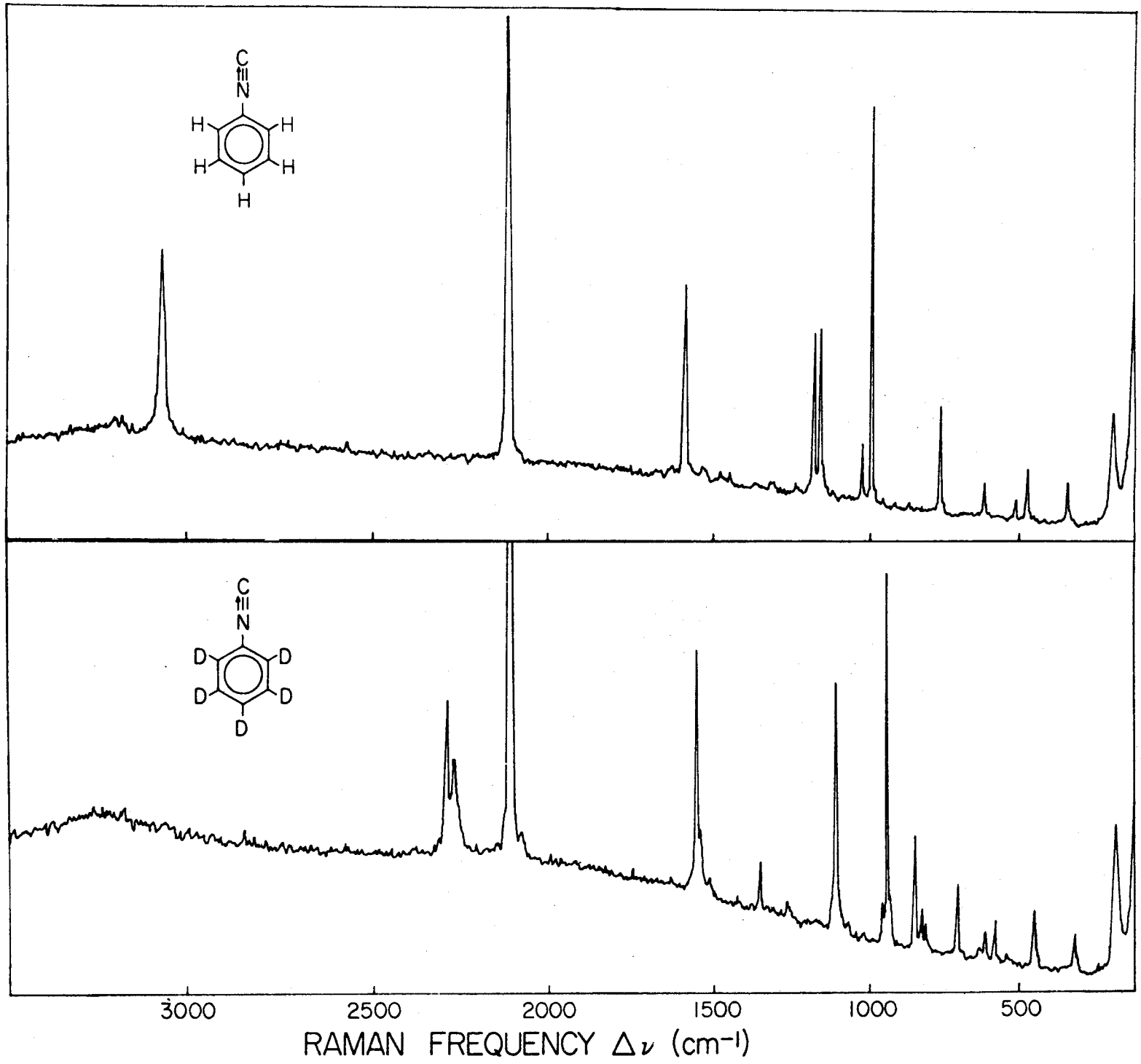
C≡N
H
H
H
H
H
C≡N
D
D
D
D
D
3000
2500
2000
1500
1000
500
RAMAN FREQUENCY Δν (cm⁻¹)

The analysis is now presented in more detail.

1. C-C Stretches

All five fundamentals ν_5 (k), ν_6 (m), ν_{25} (l), ν_{26} (n) and ν_{27} (o) appear as sharp bands in the infrared with very strong or medium intensity. The only one of these having strong intensity in the Raman is ν_5. Although it is a_1 it has a rather high depolarization ratio of 0.57.

The modes of ν_5 and ν_{25} both appear in the infrared as very sharp distinct bands at 1593 cm^{-1} and 1587 cm^{-1} respectively. Thus one might argue that since only one of these, ν_5, is seen in the Raman the other mode, ν_{25}, might be hidden under ν_5 and be raising the depolarization ratio since ν_{25} is non-totally symmetric. However, similar behaviour in the depolarization of ν_5 has been observed for C_6H_5CCH where both these modes appear in the Raman. The depolarization ratio helps to distinguish ν_5 from ν_{25}.

The intensity of ν_6 in the Raman for C_6H_5NC increases quite significantly for C_6D_5NC and it is expected that deuteration will lower its frequency by a large amount. This was found to be true as it dropped to 1368 cm^{-1} upon deuteration with a depolarization ratio of 0.20.

The assignment of ν_{26} and ν_{27} is straightforward by looking at their expected ranges.

2(a). Skeletal (In Plane)

The vibrations in this group correspond to ν_{10} (p), ν_{11} (r), ν_{12} (t) and ν_{31} (s).

The mode ν_{10} called the ring breating mode is expected to give an extremely strong polarized band in the Raman[43]. Thus the intense Raman band at 995 cm^{-1} in the Raman and the weak infrared band at 1001 cm^{-1} are assigned as the mode ν_{10}. These values obtained should be contrasted with that of 963 cm^{-1} in the gas phase found by Muirhead et al[13]. This value of 963 cm^{-1} seems to be too low. The ring breathing mode was reported to be at 998 cm^{-1} for C_6H_5CCH[4] and at 1001 cm^{-1} for C_6H_5CN[7].

The mode ν_{11} is distinguished from ν_{18} by the large drop in frequency experienced by ν_{18} upon deuteration and also by their depolarization ratios.

The vibration ν_{12} is easily assigned as it is the only polarized band in the appropriate region.

Mode ν_{31} appears at 613 cm^{-1} in the Raman and has a depolarization value of 0.75. Muirhead et al[13] do not see this band in their gas phase infrared work but report an excited state value of 547 cm^{-1}. Furthermore this vibration is prominent in the fluorescence of C_6H_5NC[46] as a false origin, just as for C_6H_5CCH[5].

2(b). Skeletal (Out of Plane)

The vibrations comprising this group are ν_{15} (w), ν_{19} (v), and ν_{20} (x).

Vibration ν_{15} of a_2 symmetry here is usually found in the 400 cm^{-1} region as a very weak band. Consequently the very weak infrared band at 418 cm^{-1} is assigned as ν_{15}. Its corresponding frequency in C_6D_5NC

is estimated from the belief that the weak infrared band at 739 cm^{-1} is an overtone, $2\nu_{15}$. Mode ν_{15} also appears in the phosphorescence of C_6D_5NC[46] at 360 cm^{-1}.

Mode ν_{19} appears in the region 680 cm^{-1} to 700 cm^{-1}. Thus the very strong band at 680 cm^{-1} in the infrared is assigned as ν_{19}.

Vibration ν_{20} is an X-sensitive vibration whose expected frequency range is 430 cm^{-1} to 560 cm^{-1}. A substantial decrease in frequency upon ring deuteration is expected for this mode. The band at 469 cm^{-1} has a depolarization ratio of 0.20. The band at 478 cm^{-1} changes very little upon deuteration. Therefore the strong infrared band at 512 cm^{-1} is assigned as ν_{20}. The frequency is found to drop to 452 cm^{-1} upon deuteration. The comparable strong infrared bands for C_6H_5CCH and C_6H_5CN are found at 530 cm^{-1} and 548 cm^{-1}, respectively. Deuteration lowers the frequency of this vibration by 60 cm^{-1} for all three isoelectronic molecules.

3(a). C-H Stretches

Modes ν_1, ν_2, ν_3, ν_{23}, and ν_{24} belong to this group.

The C-H stretching frequencies for monosubstituted aromatics lie in the range 3010 cm^{-1} to 3120 cm^{-1}. The region around 3000 cm^{-1} in the vibrational spectra of monosubstituted benzenes is not well resolved. This is due to the fact that both C-H stretches and combination bands such as $\nu_5 + \nu_6$; $\nu_5 + \nu_{26}$; $\nu_6 + \nu_{25}$; $\nu_{25} + \nu_{26}$, occur in this region. Although all five modes are allowed in the infrared and Raman, only three bands are usually discernable in the infrared[47].

For monosubstituted benzenes the strongest infrared band in this region is usually taken as ν_{24}, at 3067 cm^{-1} for C_6H_5NC, while the only prominent Raman band is suggested to be ν_2 at 3071 cm^{-1} with $\rho = 0.19$. A weak Raman band at 3044 cm^{-1}, at 3046 cm^{-1} in the infrared, is assigned as ν_3. The broad strong infrared band in the 3100 cm^{-1} region has several shoulders. The assignments for ν_1 and ν_{23} are tentative and could possibly be reversed.

These five stretching modes are expected in the neighbourhood of 2280 cm^{-1} upon deuteration. For C_6D_5NC there is one strong infrared band in this region at 2283 cm^{-1} which by analogy with C_6H_5NC has been assigned as ν_{24}. However, a medium band in the Raman with $\rho = 0.42$ at 2285 cm^{-1} suggests an a_1 band also. The rather high depolarization ratio for this band might be caused by an underlying ν_{23} mode. The most intense Raman band at 2303 cm^{-1} with $\rho = 0.13$ is assigned as an a_1 C-D stretch, ν_1. Since only one other shoulder is observed in the infrared at 2260 cm^{-1}, it seems possible that both ν_3 and ν_{24} are there. Note that the C-H and C-D stretches are listed in Table 4.4 in order of decreasing frequency and no correlation is intended between the two molecules for these particular modes.

3(b). C-H (In Plane)

This group consists of ν_8 (a), ν_9 (b), ν_{28} (e), ν_{29} (c), ν_{30} (d).

Two of them, ν_8 and ν_9, are expected to be prominent in the Raman and this was observed for C_6H_5NC. Vibration ν_8 is expected to appear in

the range 1170 cm^{-1} to 1181 cm^{-1}. There is also expected to be a large decrease in frequency upon substitution, 860 cm^{-1} to 880 cm^{-1}. The very strong band at 1167 cm^{-1} in the infrared is assigned as ν_8. It is also observed in the Raman at 1160 cm^{-1} with $\rho = 0.11$. It shifts to 863 cm^{-1} upon deuteration. This mode ν_8 undergoes a substantial change in intensity in the infrared upon deuteration, going from very strong in C_6H_5NC to weak in C_6D_5NC.

The strong infrared band at 1028 cm^{-1} and Raman band at 1025 cm^{-1} with $\rho = 0.06$ is assigned as ν_9. The frequency drops to 826 cm^{-1} in C_6D_5NC. The very strong band in the infrared at 1288 cm^{-1} is assigned as ν_{28}. The corresponding frequency for C_6H_5CCH is 1282 cm^{-1} (weak) and 1289 cm^{-1} (strong) for C_6H_5CN.

The mode ν_{29} is assigned to the shoulder at 1162 cm^{-1} in the infrared and 1153 cm^{-1} shoulder in the Raman. This mode is differentiated from ν_8 by the value of the depolarization ratio obtained for ν_8.

The range for ν_{30} is 1065 cm^{-1} to 1082 cm^{-1}. Thus the very strong infrared band at 1070 cm^{-1} is assigned to ν_{30}.

3(c). C-H (Out of Plane

These include vibrations ν_{13} (h), ν_{14} (g), ν_{16} (j), ν_{17} (i) and ν_{18} (f).

The expected frequency range for ν_{17} is 882 cm^{-1} to 938 cm^{-1}. There is only one band in this range. Thus the very strong infrared band at 914 cm^{-1} is assigned to ν_{17}.

Mode ν_{18}, the "umbrella" vibration is found between 728 cm^{-1} and 797 cm^{-1}. The very strong infrared band at 753 cm^{-1} is assigned as ν_{18}. This mode is known to give very strong infrared absorption[43].

The other b_1 mode, ν_{16}, lies between 973 cm^{-1} and 985 cm^{-1}. The weak infrared band at 989 cm^{-1} is assigned as ν_{16}. It is found at 985 cm^{-1} for C_6H_5CCH and is estimated to be at 989 cm^{-1} for C_6H_5CN. This mode undergoes a large decrease in frequency upon deuteration. The Raman band at 847 cm^{-1} for C_6D_5NC is assigned to ν_{16}. It is interesting to note that this vibration is not seen in the infrared for C_6D_5NC, C_6D_5CCH or C_6D_5CN.

The assignments for the two a_2, C-H out of plane vibrations ν_{13} and ν_{14} are straightforward because in each case there was only one band found which falls in the appropriate range. The assignment of ν_{13} and ν_{14} is aided by the fact that these two fundamentals appear in combination bands with ν_{16}, ν_{17} and ν_{18} which are of medium to strong intensity in the 1650 cm^{-1} to 2000 cm^{-1} region of the infrared[42]. This is a very characteristic region, and has been used to identify substitution types[48]. An explanation of why ν_{13} and ν_{14} give rise to combination bands of medium to strong intensity when they themselves should be infrared inactive may be found in reference (42).

4(a). C-X (Stretch)

The expected range for this mode, ν_7 (q), is 1100 cm^{-1} to 1280 cm^{-1}. The band at 1188 cm^{-1} (very strong) and medium intensity Raman band at 1183 cm^{-1} with $\rho = 0.20$ is assigned as ν_7. The mode is distinguished from

ν_{29} by its depolarization ratio and from ν_8 by the large decrease in frequency upon deuteration for ν_8. Muirhead et al[13] report seeing this mode in the gas phase infrared at 1186 cm^{-1}.

4(b). C-X (In Plane)

This vibration ν_{33} (u) is generally weak in the Raman, and has an expected frequency range of 200 cm^{-1} to 410 cm^{-1}. Thus the weak Raman band at 325 cm^{-1} is assigned as the in plane C-X band, ν_{33}. This band was found to have a rather high depolarization ratio which is strong evidence against a possible 2 x 162 cm^{-1} assignment. Vibration ν_{33} is influenced by both the mass of the substituent and its binding strength to the ring. This frequency for C_6H_5NC is lower than for either C_6H_5CCH, 349 cm^{-1} or C_6H_5CN, 381 cm^{-1}. The masses of all the substituents are nearly equal. Thus differences in frequency could arise out of the differences in bonding to the ring.

4(c). C-X (Out of Plane)

The frequency range for ν_{22} (y) is 140 cm^{-1} to 250 cm^{-1} and is usually quite strong in the Raman. Thus ν_{22} is assigned to the 162 cm^{-1} depolarized Raman band.

5(a). N≡C (Stretch)

In aliphatic isonitriles the nitrogen-carbon stretch of the substituent is found at 2140 cm^{-1}[15], while in aromatic isonitriles this value falls to 2120 cm^{-1}. The infrared and Raman bands at 2125 cm^{-1}

and 2124 cm^{-1} with a $\rho = 0.25$ are thus attributed to ν_4.

5(b). $\beta N\equiv C$

The internal in plane band of the NC group, ν_{32}, is assigned to the strong infrared band at 478 cm^{-1}. It is distinguished from the band at 469 cm^{-1} by the latter's depolarization ratio. The corresponding modes in C_6H_5CCH and C_6H_5CN appear strongly in the infrared at 513 cm^{-1} and 551 cm^{-1} respectively. In addition, the fluorescence of C_6H_5NC[46] and C_6H_5CCH[5] show this vibration as another false origin. The excited electronic state frequency of ν_{32} for C_6H_5NC in the gas phase has been assigned the value of 452 cm^{-1}[13]. In Reference (13) a band at 475 cm^{-1} to the red of the assigned (0,0) was seen. It was assumed to be ν_{32} and this work now verifies that assumption.

5(c). $\gamma N\equiv C$

An unsuccessful attempt was made to split the Raman band at 162 cm^{-1}. However, for C_6H_5CN such a low frequency Raman band was able to be split and one of the corresponding split bands was assigned as the out of plane internal CN band[49]. Also in this work, no unassigned bands remain in the low frequency region. Thus the out of plane internal NC band, ν_{21}, is assumed to lie under ν_{33} at 325 cm^{-1}. An alternate approach would be to assume that ν_{21} is hidden under the 162 cm^{-1} band. However, in this case one would expect to find Fermi Resonance between the two modes which would cause them to split.

Assignments for the deuterated molecule fit very well with the deuterium shifts found for benzonitrile[7,8] and ethynylbenzene[4].

The Teller-Redlich product ratio was calculated for the a_1 modes. The observed value of 0.186 agrees well with the calculated value of 0.181 and thus supports the assignments made for the a_1 modes.

TABLE 4.3

Frequencies (cm^{-1}) and Assignments for Infrared and Raman Bands of C_6H_5NC and C_6D_5NC

C_6H_5NC			C_6D_5NC		
IR	Raman (ρ)	Assignment	IR	Raman (ρ)	Assignment
	162(0.83)	ν_{22}		160(0.80)	ν_{22}
325 vw	325(0.77)	ν_{21},ν_{33}		311	ν_{21},ν_{33}
418 vw		ν_{15}	452 vs	449	ν_{20}
472 s	467(0.20)	ν_{12}	461 sh	456(0.32)	ν_{12}
478 vs		ν_{32}	471 sh		ν_{32}
512 vs	510(0.65)	ν_{20}	550 vs	551	ν_{19}
617 sh	613(0.75)	ν_{31}	572 m		$\nu_{28}-\nu_{12}$
664 s		$\nu_{20}+\nu_{22}$	598 m	592(0.76)	ν_{31}
680 vs		ν_{19}	629 vs	627(0.78)	ν_{18}
753 vs	754 sh	ν_{18}	654 m	645	$\nu_{10}-\nu_{33}$
763 sh	761(0.07)	ν_{11}	674 m		$\nu_{15}+\nu_{33}$
809 vw		$\nu_{32}+\nu_{33}$	696 w		ν_{14}
840 m		ν_{14}	722 vs	719(0.07)	ν_{11}
882 w		$\nu_{15}+\nu_{32}$	739 w		$2\nu_{15}$
914 vs		ν_{17}	763 vs		ν_{17}
967 w		ν_{13}	787 vw		$\nu_{18}+\nu_{22}$
989 w	985 sh	ν_{16}	817 s		ν_{30}
1001 w	995(0.03)	ν_{10}	830 m	823(0.10)	ν_{9}
1014 m		$2\nu_{20}$	844 m	841(0.85)	ν_{29}
1028 s	1025(0.06)	ν_{9}		847	ν_{16}
1070 vs	1066	ν_{30}	866 w	861(0.11)	ν_{8}
1098 m		$\nu_{15}+\nu_{19}$	889 vw		$\nu_{11}+\nu_{22}$
	1116	$\nu_{20}+\nu_{31}$	903 m		$2\nu_{20}$
1162 sh	1153 sh	ν_{29}	927 w		$2\nu_{12}$
1167 vs	1160(0.11)	ν_{8}	935 w		$\nu_{12}+\nu_{32}$
1188 vs	1183(0.20)	ν_{7}	951 vw		$2\nu_{32}$
1242 m	1241	$\nu_{11}+\nu_{32}$	962 m	957(0.03)	ν_{10}
1288 vs		ν_{28}		968	$\nu_{15}+\nu_{31}$
1311 m		$\nu_{14}+\nu_{32}$	1001 vw	1002	$\nu_{19}+\nu_{20}$
1328 m	1325	ν_{27}	1036 m	1036	ν_{28}

Table 4.3 (continued)

C_6H_5NC			C_6D_5NC		
IR	Raman (ρ)	Assignment	IR	Raman (ρ)	Assignment
1394 w		$\nu_{12}+\nu_{17}$	1059 vw		$\nu_{12}+\nu_{31}$
1429 m		$\nu_{18}+\nu_{19}$	1106 m		$2\nu_{19}$
1454 vs	1452	ν_{26}	1127 vs	1120 (0.08)	ν_7
1485 vs	1485	ν_6	1141 s		$\nu_{14}+\nu_{20}$
1500 vs		$2\nu_{18}$	1157 vs		$\nu_{29}+\nu_{33}$
	1533	$2\nu_{11}$	1180 m	1190	$\nu_{18}+\nu_{19}$
1587 vs		ν_{25}	1236 s		$\nu_{14}+\nu_{19}$
1593 vs	1597 (0.57)	ν_5	1283 m	1281	ν_{27}
1638 w		$\nu_8+\nu_{12}$	1319 m		$\nu_{14}+\nu_{18}$
1648 w		$\nu_8+\nu_{32}$	1334 m	1332	ν_{26}
1673 m		$\nu_{17}+\nu_{18}$	1350 m		$\nu_{11}+\nu_{18}$
1752 m		$\nu_{14}+\nu_{17}$	1369 vs	1368 (0.20)	ν_6
1800 m		$\nu_{13}+\nu_{14}$	1395 m		$\nu_{17}+\nu_{18}$
1882 m		$\nu_{13}+\nu_{17}$	1408 m		$\nu_{10}+\nu_{20}$
1956 s		$\nu_{13}+\nu_{16}$	1415 m		$\nu_8+\nu_{19}$
2068 m		$\nu_5+\nu_{32}$	1435 w		$\nu_9+\nu_{31}$
2092 s		$\nu_9+\nu_{30}$	1445 w		$2\nu_{11}$
2125 vs	2125 (0.25)	ν_4	1454 w		$\nu_{14}+\nu_{17}$
2192 w		$\nu_8+\nu_9$	1467 w		$\nu_{13}+\nu_{14}$
2238 w		$\nu_6+\nu_{18}$	1500 vw		$\nu_8+\nu_{18}$
2255 m		$\nu_7+\nu_{30}$	1522 vw		$\nu_{13}+\nu_{17}$
2284 s		$\nu_{10}+\nu_{28}$	1554 m	1552	ν_{25}
2328 sh		$\nu_8+\nu_{29}$	1565 vs	1561 (0.52)	ν_5
2336 vs		$2\nu_8$	1588 m		$\nu_8+\nu_{11}$
2455 m		$\nu_8+\nu_{28}$	1613 m		$\nu_{13}+\nu_{16}$
2524 vw		$\nu_{26}+\nu_{30}$	1640 vs	1641	$2\nu_{30}$
2554 vw		$\nu_6+\nu_{30}$	1720 w		$\nu_7+\nu_{31}$
2598 w		$\nu_4+\nu_{12}$	1736 w		$2\nu_8$
2622 w		$\nu_8+\nu_{26}$	1808 vw		$\nu_{26}+\nu_{32}$
2642 w		$\nu_7+\nu_{26}$	1854 vw		$\nu_7+\nu_{11}$

Table 4.3 (continued)

C_6H_5NC			C_6D_5NC		
IR	Raman (ρ)	Assignment	IR	Raman (ρ)	Assignment
2674 vw		$\nu_6+\nu_7$	1869 vw		$\nu_9+\nu_{28}$
2756 w		$\nu_8+\nu_{25}$	1962 w		$\nu_7+\nu_9$
2779 vw		$\nu_5+\nu_7$	2026 vw		$\nu_5+\nu_{12}$
2798 vw		$\nu_4+\nu_{19}$	2090 s	2089 (0.33)	$\nu_6+\nu_{11}$
2908 m		$2\nu_{26}$	2124 vs	2122 (0.25)	ν_4
2938 m		$\nu_6+\nu_{26}$	2197 vw		$\nu_5+\nu_{18}$
2968 m	2966	$2\nu_6$	2262 sh		ν_3, ν_{24}
3046 s	3044	ν_3	2283 s	2285 (0.42)	ν_2, ν_{23}
3067 vs	3066 sh	ν_{24}	2304 sh	2303 (0.13)	ν_1
3075 sh	3071 (0.19)	ν_2	2374 vw		$\nu_5+\nu_{30}$
3089 sh		ν_1	2439 w		$\nu_4+\nu_{33}$
3105 sh		ν_{23}	2584 w		$\nu_4+\nu_{20}$
3186 m		$2\nu_5$	2650 vw		$\nu_6+\nu_{27}$
			2689 vw		$\nu_5+\nu_7$
			2756 vw		$\nu_4+\nu_{18}$
			2877 w		$\nu_4+\nu_{17}$
			2932 m		$\nu_5+\nu_6$
			2980 m		$\nu_4+\nu_8$
			3061 vw		$\nu_2+\nu_{17}$
			3117 vw		$\nu_5+\nu_{25}$
			3246 w		$\nu_4+\nu_7$

TABLE 4.4

Ground State Fundamentals of Phenyl Isocyanides

Symmetry	Designation	Description of C_6H_5NC Mode[a]		Frequency, (cm^{-1})	
				C_6H_5NC	C_6D_5NC
a_1	ν_1	νC-H		3089	2303
	ν_2	νC-H		3071	2283
	ν_3	νC-H		3046	2262
	ν_4	νN≡C		2125	2123
	ν_5	νC-C	k 8a	1595	1565
	ν_6	νC-C	m 19a	1485	1368
	ν_7	χ-sens (νC-NC)	q 13	1185	1123
	ν_8	βC-H	a 9a	1163	863
	ν_9	βC-H	b 18a	1026	826
	ν_{10}	RING	p 12	998	959
	ν_{11}	χ-sens (αC-C-C)	r 1	762	720
	ν_{12}	χ-sens (αC-C-C)	t 6a	469	456
a_2	ν_{13}	γC-H	h 17a	967	(767)[b]
	ν_{14}	γC-H	g 10a	840	696
	ν_{15}	φC-C	w 16a	418	(370)[b]
b_1	ν_{16}	γC-H	j 5	989	847
	ν_{17}	γC-H	i 17b	914	763
	ν_{18}	γC-H	f 11	753	628
	ν_{19}	φC-C	v 4	680	550
	ν_{20}	χ-sens (φC-C)	x 16b	512	452
	ν_{21}	γN≡C		325	311
	ν_{22}	χ-sens (γC-NC)	y 10b	162	160

Table 4.4 (continued)

Symmetry	Designation	Description of C_6H_5NC Mode[a]		Frequency, (cm^{-1})	
				C_6H_5NC	C_6D_5NC
b_2	ν_{23}	νC-H		3105	2283
	ν_{24}	νC-H		3067	2262
	ν_{25}	νC-C	l 8b	1587	1554
	ν_{26}	νC-C	n 19b	1454	1334
	ν_{27}	νC-C	o 14	1328	1283
	ν_{28}	βC-H	e 3	1288	1036
	ν_{29}	βC-H	c 15	1157	842
	ν_{30}	βC-H	d 18b	1070	817
	ν_{31}	αC-C-C	s 6b	613	595
	ν_{32}	βN≡C		478	471
	ν_{33}	χ-sens (βC-NC)	u 9b	325	311

a. The second column under this heading correlates the vibrational modes of the phenyl isocyanides with the labelling of the vibrational modes of monosubstituted benzenes by Whiffen[43]. The third column lists the corresponding mode in benzene, according to Wilson[62].

b. Estimated value.

CHAPTER V

PHOSPHORESCENCE AND FLUORESCENCE ANALYSIS

5.1 Phosphorescence

Ground state fundamentals of C_6H_5NC and C_6D_5NC used in this analysis are found in Table 4.4. Phosphorescence spectra of 10^{-3} M C_6H_5NC and C_6D_5NC in polycrystalline methylcyclohexane at 77°K are shown in Figures 5.1 and 5.2. These spectra were found to be much better resolved than when methylcyclohexane glass was used.

Martin and Kalantar[50] have noted cooling methylcyclohexane produces both a glass and polycrystalline matrix. Figure 5.3 shows phosphorescence emission in the case when there is a large contribution from both emission in the glass and in the polycrystalline matrix environment. Note the sharpness of the bands corresponding to emission from a polycrystalline matrix (bands to the blue) as compared to those from a glass (bands to the red). The (0,0) band of polycrystalline matrix emission is separated by 155 cm^{-1} to the blue from the (0,0) band of glass emission.

The extreme cases when there is emission essentially from one environment or the other is also observed.

In these phosphorescence studies of C_6H_5NC and C_6D_5NC in polycrystalline methycyclohexane no splitting of the (0,0) band and other prominent bands was observed. This was also true of C_6H_5CCH. However,

C_6H_5CN showed splittings of 60 cm^{-1} in both phosphorescence and fluorescence in polycrystalline methylcyclohexane and was attributed to emission from two different orientations in a single crystalline modification of the solvent. This type of splitting is to be contrasted with that shown in Figure 5.3. It is perhaps interesting to note that although splittings of the type described above for the fluorescence and phosphorescence of C_6H_5CN were not observed in the phosphorescence of C_6H_5NC, they were seen in the fluorescence spectra of this molecule.

The emission in the phosphorescence spectra produced by broad band excitation into the first singlet state is analyzed in Tables 5.1 and 5.2. Since all the luminescence spectra were taken at 77°K, at which temperature kT equals 54 cm^{-1}, no appreciable population in vibrationally excited S_1 and T_1 is expected. The phosphorescence spectra of C_6H_5NC and C_6D_5NC are similar but quite distinct from their fluorescence spectra. As is the case with the phosphorescence spectra of C_6H_5CN[9] and C_6H_5CCH[6] the two most intense bands for C_6H_5NC are the ν_5, the C-C stretching of the ring and the (0,0) band.

The very strong band at 27,190 cm^{-1} (a broad band at 27,035 cm^{-1} in the glass) is assigned as the (0,0) transition. The strong intensity of the (0,0) indicates the orbit allowedness of the triplet-singlet transition by comparison with the intensity of the (0,0) of phosphorescence for C_6H_5CCH[6] and C_6H_5CN[9]. The (0,0) of phosphorescence was established to be the true (0,0) of the transition $T_1 \rightarrow S_0$ for these molecules by comparison with singlet-triplet absorption by oxygen perturbation[51].

The fundamentals ν_4, ν_5, ν_7, ν_8, ν_9, ν_{10}, ν_{11}, ν_{12}, ν_{20}, ν_{22} and ν_{33} appear in the phosphorescence spectrum of C_6H_5NC at 2125, 1595, 1190, 1160, 1025, 1005, 775, 480, 500, 165, 330 cm^{-1} respectively. Of these all are a_1 except ν_{20} and ν_{22} which are b_1, and ν_{33} which is b_2. These three nontotally symmetric vibrations are of weak intensity which suggests that vibrational perturbations are very small. To account for their appearance, means of combining spin-orbit and vibrational effects must be considered. These include spin-vibronic coupling, vibronic coupling among triplets with spin-orbit coupling, and vibronic coupling among singlets with spin-orbit coupling. Each of these predict that b_1 vibrations may be observed in the spectra due to $^1A_1$ (z) and $^1B_2$ (y) singlet admixture, and b_2 vibrations due to $^1A_1$ (z) and $^1B_1$ (x) mixing. However, these three mechanisms cannot be distinguished experimentally.

The weak band at 165 cm^{-1} is assigned as ν_{22}. For C_6H_5CCH a broad very weak band is seen at 190 cm^{-1} in the fluorescence, whose shape varies from one experiment to another, and is believed to be a lattice mode. However, the band at 165 cm^{-1} here is very sharp and it is believed to be a genuine fundamental of C_6H_5NC.

The very weak band assigned as ν_{33} at 330 cm^{-1} may be serving as a false origin, but the only bands suggested to be based on it are broad or shoulders, and play a very insignificant part in the overall spectrum. The main progression is in the 1595 cm^{-1} totally symmetric C-C stretching vibration, ν_5. Almost all the combination bands involve this mode also. This progression is interpreted as indicative of a planar, non-regular hexagon benzene ring geometry of the lowest triplet state. The

resolution of the spectra here does not permit one to do a reduced intensity calculation on the various members of a progression to obtain a quantitative answer to the change in geometry.

On perdeuteration the (0,0) blue shifts 110 cm^{-1} to 27,300 cm^{-1}. Shifts of 100 cm^{-1} for C_6H_5CN in methylcyclohexane and 85 cm^{-1} for C_6H_5CCH in isopentane on deuteration have been reported. Vibration ν_{20} expected at about 450 cm^{-1} for C_6D_5NC is not seen in the spectrum of the perdeuterated molecule and may be hidden under ν_{12} at 470 cm^{-1}. The 1025 cm^{-1} shoulder in C_6H_5NC denoted by ν_9, expected at about 825 cm^{-1} in C_6D_5NC is probably very weak and/or masked by the medium band at 875 cm^{-1}. Vibrations ν_6 (a_1), ν_{15} (a_2) and ν_{19} (b_1) not seen in the phosphorescence of C_6H_5NC appear in that of C_6D_5NC. The other fundamentals appearing in C_6D_5NC are the same as those of C_6H_5NC. Thus fundamentals appear at 170, 300, 360, 470, 560, 725, 875, 965, 1135, 1380, 1575, 2130 cm^{-1}. The frequencies of the observed bands fit well with the deuterium shifts expected for the C_6H_5NC proposed assignment. The main progression is again found to be in ν_5.

The broad background present under all the main bands for both spectra may be due to unresolved multiplet structure due to various orientations of the solute, or to lattice vibrations.

Thus C_6H_5NC with its main progression in ν_5 differs from the phosphorescence of benzene which has its main progression in ν_{10}, the ring breathing mode. The phosphorescence spectra of C_6H_5NC, C_6H_5CN and C_6H_5CCH are very similar.

Figure 5.1

Phosphorescence spectrum of phenyl isocyanide in polycrystalline methylcyclohexane at $77^{o}K$

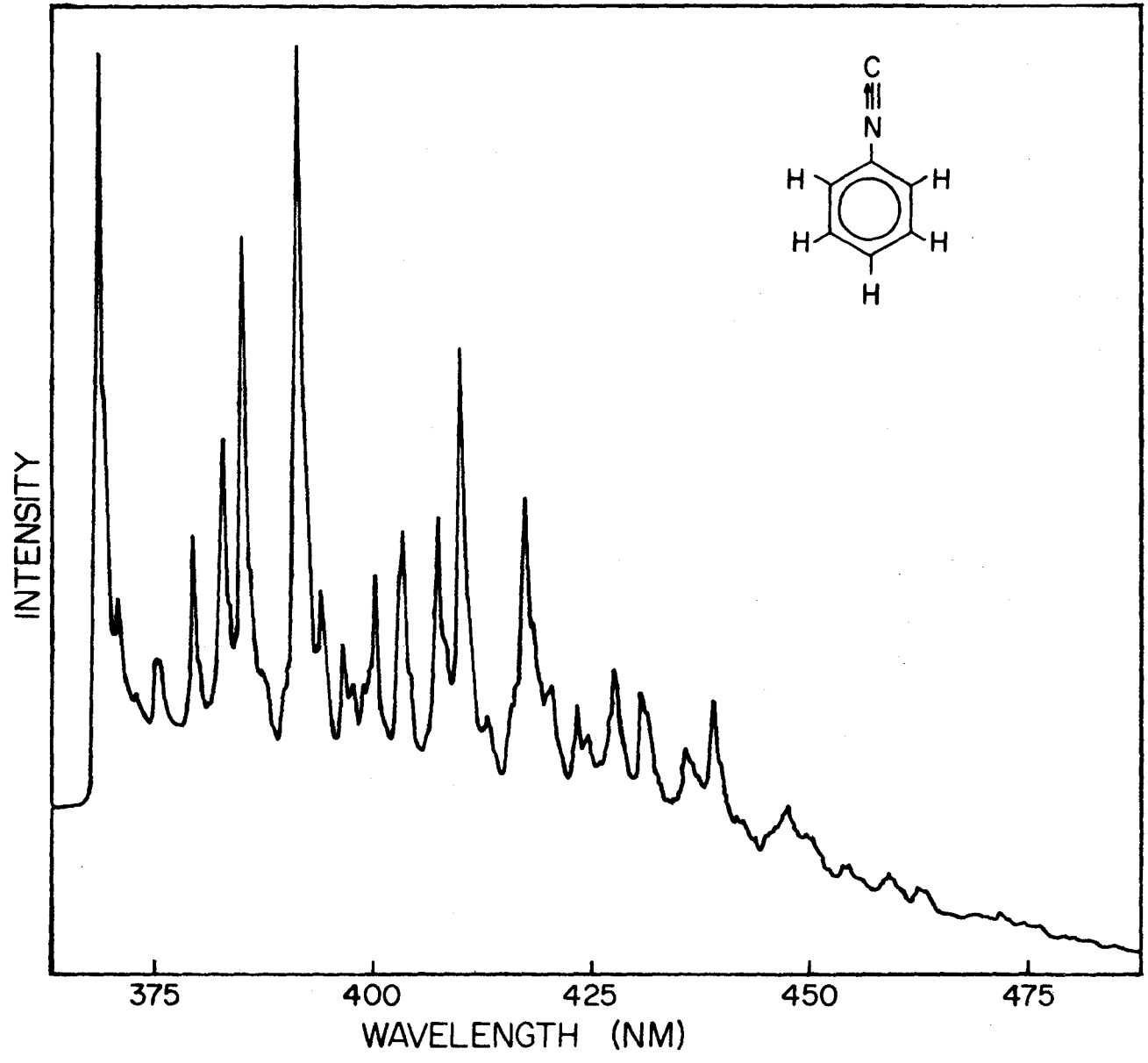
INTENSITY
375
400
425
450
475
WAVELENGTH (NM)
C
N
H
H
H
H
H

TABLE 5.1

Vibrational Analysis of the Phosphorescence Spectrum of 10^{-3}M C_6H_5NC in Polycrystalline Methylcyclohexane at 77°K

Intensity[a]	Position[b]		$\Delta\nu$ (cm^{-1})	Assignment[c]
	λ(nm x 10)	ν (cm^{-1})		
vs	3678	27,190	0	0, 0
w	3700	27,025	165	0, ν_{22}
vw	3723	26,860	330	0, ν_{33}
w	3744	26,710	480	0, ν_{12}
w	3747	26,690	500	0, ν_{20}
m	3786	26,415	775	0, ν_{11}
w	3792 sh[d]	26,370	820	0, $\nu_{12} + \nu_{33}$
m	3819	26,185	1005	0, ν_{10}
m	3822 sh	26,165	1025	0, ν_9
s	3842	26,030	1160	0, ν_8
m	3846 sh	26,000	1190	0, ν_7
m	3851 sh	25,965	1225	0, $\nu_{11} + \nu_{12}$
w	3865	25,875	1315	0, $\nu_{10} + \nu_{33}$
w	3893 sh	25,685	1505	0, $\nu_{10} + \nu_{12}$
vs	3907	25,595	1595	0, ν_5
m	3912 sh	25,560	1630	0, $\nu_8 + \nu_{12}$
w	3935	25,415	1775	0, $\nu_{10} + \nu_{11}$
w	3959	25,260	1930	0, $\nu_8 + \nu_{11}$
w	3971	25,185	2005	0, $2\nu_{10}$
w	3984	25,100	2090	0, $\nu_5 + \nu_{12}$
w	3990	25,065	2125	0, ν_4
m	3996	25,025	2165	0, $\nu_8 + \nu_{10}$
m	4024 sh	24,850	2340	0, $2\nu_8$
m	4029	24,820	2370	0, $\nu_5 + \nu_{11}$
m	4067	24,590	2600	0, $\nu_5 + \nu_{10}$

Table 5.1 (continued)

Intensity[a]	Position[b]		$\Delta\nu(cm^{-1})$	Assignment[c]
	λ(nm x 10)	ν (cm^{-1})		
s	4093	24,430	2760	0, $\nu_5 + \nu_8$
w	4124	24,250	2940	0, $\nu_8 + \nu_{10} + \nu_{11}$
w	4153 sh	24,080	3110	0, $2\nu_8 + \nu_{11}$
w	4158 sh	24,050	3140	0, $\nu_5 + 2\nu_{11}$
m	4169	23,985	3205	0, $2\nu_5$
w	4174 sh	23,960	3230	0, $\nu_5 + \nu_8 + \nu_{12}$
w	4195	23,840	3350	0, $\nu_5 + \nu_{10} + \nu_{11}$
w	4228	23,650	3540	0, $\nu_5 + \nu_8 + \nu_{11}$
vw	4239	23,590	3600	0, $\nu_5 + 2\nu_{10}$
vw	4253	23,515	3675	0, $2\nu_5 + \nu_{12}$
vw	4264 sh	23,450	3740	0, $\nu_4 + \nu_5$
w	4270	23,420	3770	0, $\nu_5 + \nu_8 + \nu_{10}$
w	4298	23,265	3925	0, $\nu_5 + 2\nu_8$
w	4305	23,230	3960	0, $2\nu_5 + \nu_{11}$
vw	4343	23,025	4165	0, $2\nu_5 + 2\nu_{12}$
w	4348	23,000	4190	0, $2\nu_5 + \nu_{10}$
w	4380	22,830	4360	0, $2\nu_5 + \nu_8$
vw	4397	22,745	4445	0, $\nu_4 + 2\nu_8$
vw	4441	22,515	4675	0, $2\nu_5 + \nu_{10} + \nu_{12}$
vw	4445	22,445	4745	0, $2\nu_5 + 2\nu_{11}$
w	4466	22,390	4800	0, $3\nu_5$
vw	4505 sh	22,200	4990	0, $2\nu_5 + \nu_{10} + \nu_{11}$
vw	4533	22,060	5130	0, $2\nu_5 + \nu_8 + \nu_{11}$
vw	4581	21,830	5360	0, $2\nu_5 + \nu_8 + \nu_{10}$
vw	4615	21,670	5520	0, $2\nu_5 + 2\nu_8$

a Uncorrected for instrumental response; s = strong, m = medium, w = weak, v = very

b Error about $\pm$ 0.1 nm

c Numbering of the normal modes follows Herzberg

d sh = shoulder

Figure 5.2

Phosphorescence spectrum of perdeuterophenyl isocyanide in polycrystalline methylcyclohexane at 77°K

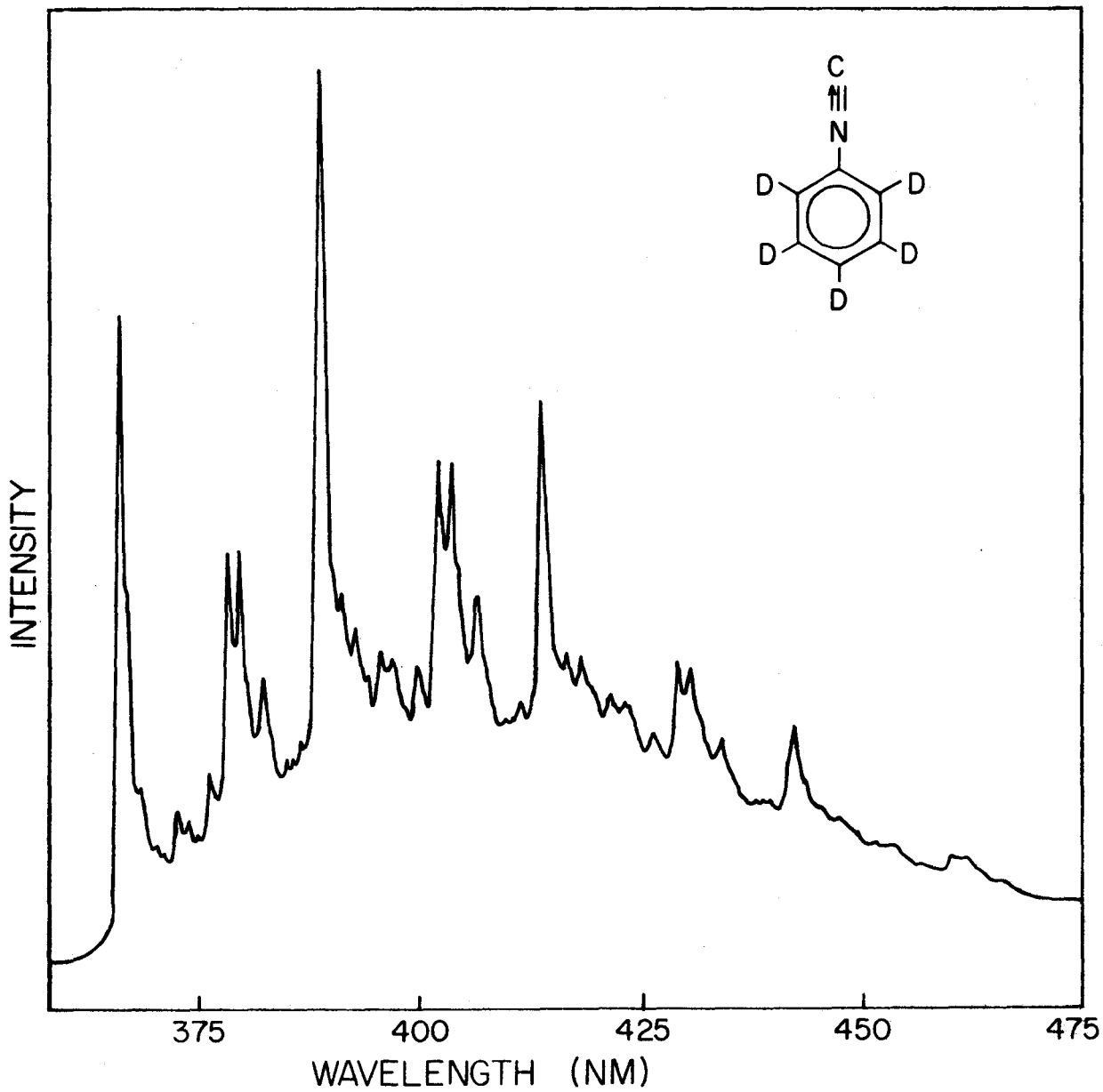
C
N
D
D
D
D
D
INTENSITY
375
400
425
450
475
WAVELENGTH (NM)

TABLE 5.2

Vibrational Analysis of the Phosphorescence Spectrum of 10^{-3}M C_6D_5NC in Polycrystalline Methylcyclohexane at 77°K

Intensity[a]	Position[b] λ(nm x 10)	Position[b] ν(cm^{-1})	Δν(cm^{-1})	Assignment[c]
s	3663	27,300	0	0, 0
w	3686	27,130	170	0, ν_{22}
vvw	3704	27,000	300	0, ν_{33}
vvw	3712	26,940	360	0, ν_{15}
vw	3727	26,830	470	0, ν_{12}
vw	3740	26,740	560	0, ν_{19}
vw	3763	26,575	725	0, ν_{11}
m	3784	26,425	875	0, ν_{8}
m	3797	26,335	965	0, ν_{10}
w	3822	26,165	1135	0, ν_{7}
vvw	3894	25,980	1320	0, $\nu_{8} + \nu_{12}$
vvw	3858	25,920	1380	0, ν_{6}
vw	3865	25,875	1425	0, $\nu_{10} + \nu_{12}$
s	3887	25,725	1575	0, ν_{5}
m	3912	25,560	1740	0, $2\nu_{8}$
w	3927	25,465	1835	0, $\nu_{8} + \nu_{10}$
w	3933 sh	25,425	1875	0, $\nu_{7} + \nu_{11}$
w	3941	25,375	1925	0, $2\nu_{10}$
w	3957	25,270	2030	0, $\nu_{5} + \nu_{12}$
w	3968	25,200	2100	0, $\nu_{7} + \nu_{10}$
w	3973	25,170	2130	0, ν_{4}
vw	3999	25,005	2295	0, ν_{5}, + ν_{11}
m	4023	24,855	2445	0, $\nu_{5} + \nu_{8}$
m	4037	24,770	2530	0, $\nu_{5} + \nu_{10}$
w	4065	24,600	2700	0, $\nu_{5} + \nu_{7}$
vw	4114	24,305	2995	0, $\nu_{5} + \nu_{10} + \nu_{12}$

Table 5.2 (continued)

Intensity[a]	Position[b] λ(nm x 10)	Position[b] ν(cm^{-1})	Δν (cm^{-1})	Assignment[c]
m	4138	24,165	3135	0, $2\nu_5$
w	4167	24,000	3300	0, $\nu_5 + 2\nu_8$
w	4185	23,895	3415	0, $\nu_5 + \nu_8 + \nu_{10}$
vw	4214	23,730	3570	0, $\nu_5 + \nu_7 + \nu_8$
vw	4218	23,710	3590	0, $2\nu_5 + \nu_{12}$
vw	4231	23,635	3665	0, $\nu_5 + \nu_7 + \nu_{10}$
vw	4238	23,595	3705	0, $\nu_4 + \nu_5$
vw	4264	23,450	3850	0, $2\nu_5 + \nu_1$
w	4292	23,300	4000	0, $2\nu_5 + \nu_8$
w	4308	23,215	4085	0, $2\nu_5 + \nu_{10}$
vw	4341	23,035	4265	0, $2\nu_5 + \nu_7$
w	4424	22,605	4695	0, $3\nu_5$
vvw	4457	22,435	4865	0, $2\nu_5 + 2\nu_8$
vvw	4475	22,345	4955	0, $2\nu_5 + \nu_8 + \nu_{10}$
vvw	4510	22,175	5125	0, $2\nu_5 + \nu_7 + \nu_8$
vvw	4539	22,030	5270	0, $\nu_4 + 2\nu_5$
vvw	4569	21,885	5415	0, $3\nu_5 + \nu_{11}$
vvw	4599	21,745	5555	0, $3\nu_5 + \nu_8$
vvw	4617	21,660	5640	0, $3\nu_5 + \nu_{10}$
vvw	4654	21,485	5815	0, $3\nu_5 + \nu_7$
vvw	4747	21,065	6235	0, $4\nu_5$

a Uncorrected for instrumental response; s = strong, m = medium, w = weak, v = very

b Error about $\pm$ 0.1 nm

c Numbering of the normal modes follows Herzberg

d sh = shoulder

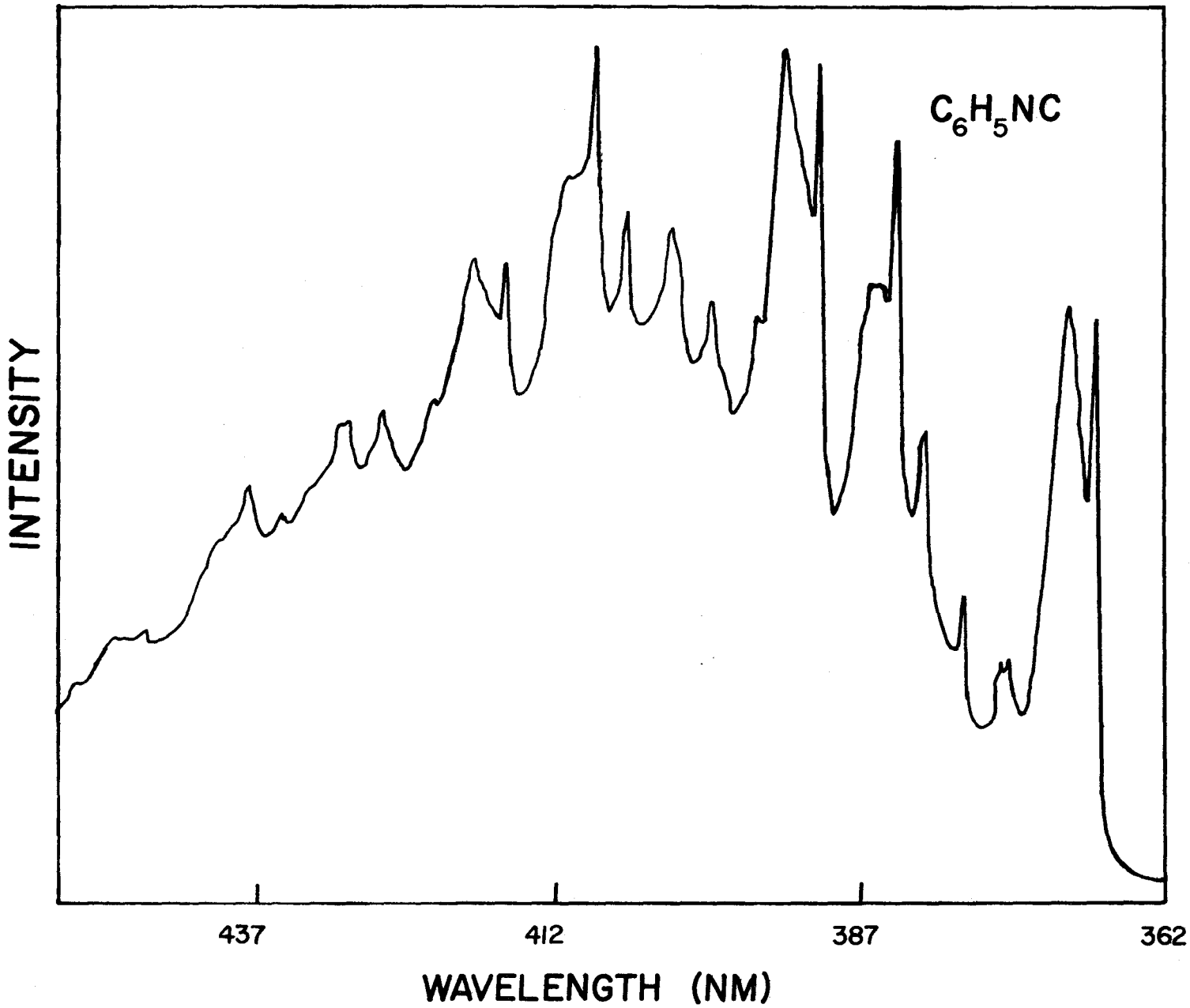

Figure 5.3 Phosphorescence of phenyl isocyanide from both glass and polycrystalline environments in methylcyclohexane at 77°K.

5.2 Assignment of the Orbital Symmetry of the Lowest Triplet State

The theory behind polarization of luminescence and the assigning of the lowest triplet state has been discussed in Sections 2.16 and 2.17.

The lowest triplet state symmetry is assigned by performing polarization measurements on the (0,0) band of the phosphorescence spectra. The intensities of the vertically and horizontally polarized emission of the (0,0) band of phosphorescence of a 10^{-3} M solution of C_6H_5NC in solutions of 80% to 20% by volume of methylcyclohexane to 3-methylpentane, and 75% to 25% of 3-methylpentane to methylcyclohexane were measured following excitation with vertically and horizontally polarized light. It is assumed here, as by Muirhead et al[13] that the symmetry of the first excited singlet state is $^1B_2$ and the second excited singlet to be $^1A_1$.

The wavelengths of excitation were 2355 $\overset{o}{A}$, and 2722 $\overset{o}{A}$ corresponding to the (0,0) region of the $^1A_1 \rightarrow {}^1B_2$ ($S_0 \rightarrow S_1$) and the $^1A_1 \rightarrow {}^1A_1$ ($S_0 \rightarrow S_2$) transitions respectively.

When exciting into the (S_0 - S_1) band the degree of polarization ranged from -2% to -10% whereas excitation into the (S_0 - S_2) band gave -13% to -25%. For a given experiment, the degree of polarization was always more negative when exciting into the (0,0) of the (S_0 - S_2) band than when exciting into the (0,0) region of the (S_0 - S_1) band, but the results from day to day varied somewhat. The above results, that the degree of polarization was less negative for the $^1A_1 \rightarrow {}^1B_2$ than for $^1A_1 \rightarrow {}^1A_1$ transition allows one to assign the orbital symmetry of the phosphorescent π-π^* state as $^3A_1$ for phenyl isocyanide of C_{2v} symmetry.

This was also found for C_6H_5CCH[6] and C_6H_5CN[9].

The polarizations of other major bands in the phosphorescence spectrum were of a similar value to that found for the (0,0) band, thus substantiating the assignment of these bands to a_1 fundamentals.

5.3 Phosphorescence Lifetimes

The phosphorescence lifetimes of 10^{-3} M solutions of C_6H_5NC and C_6D_5NC in 3-methylpentane, 95% ethanol and polycrystalline methylcyclohexane at 77°K are listed in Table 5.3.

For each species C_6H_5NC and C_6D_5NC there is a change in lifetime in going from one solvent to another. It appears that this change in lifetime with varying solvent may be correlated with the viscosity of the solvent. The viscosities of 3-methylpentane[52] and ethanol + 4% water[53] at 77°K are 2.2×10^{12} poises and 2.1×10^{19} poises respectively. Polycrystalline methylcyclohexane may be considered a solid. Thus one observes an increased lifetime with increasing viscosity of the solvent. The solvent is believed to affect the radiative part of the sum of rate constants[54], i.e., the k_{rad} of:

$$\frac{1}{\tau_{Ph}} = k_{rad} + k_{nonrad} \quad . \tag{5.1}$$

Phosphorescence lifetimes of aromatic molecules are known to increase upon deuteration. This was also observed in the case of C_6H_5NC,

TABLE 5.3

Phosphorescence Lifetimes of Phenyl Isocyanide at 77°K

Solvent	τ_{Phos} (sec)		$1/\tau_{Phos}$ (sec^{-1})	
	C_6H_5NC[a]	C_6D_5NC	C_6H_5NC	C_6D_5NC
3-Methylpentane (glass)	5.14 ± 0.12[b]	6.26 ± 0.16	0.194	0.159
Ethanol (cracked glass)	5.54 ± 0.08	6.67 ± 0.07	0.180	0.149
Methylcyclohexane (polycrystalline)	5.74 ± 0.07	6.80 ± 0.11	0.174	0.147

a. Concentrations for each solute-solvent pair were 10^{-3} M and 10^{-4} M.

b. Lifetimes are the average of at least six measurements.

as C_6D_5NC showed about a 20% increase in lifetime when compared with the lifetime of C_6H_5NC in the same solvent.

In comparing the solvent effect on the differences in the rate constants for C_6H_5NC and C_6D_5NC in a common solvent, i.e., in relating:

$$\left(\frac{1}{\tau_{Ph}}\right)^{H}_{Solv\ 1} - \left(\frac{1}{\tau_{Ph}}\right)^{D}_{Solv\ 1} \text{ with } \left(\frac{1}{\tau_{Ph}}\right)^{H}_{Solv\ 2} - \left(\frac{1}{\tau_{Ph}}\right)^{D}_{Solv\ 2}$$

where the superscripts H and D refer to C_6H_5NC and C_6D_5NC respectively, and Solv 1 and Solv 2 refer to 2 different solvents, it was found that the difference was constant to within 10%. This can be interpreted as suggestive that the deuterium effect, perturbing k_{nonrad} only, is independent of solvent.

5.4 Electronic Absorption and Fluorescence Excitation

A liquid phase electronic absorption spectrum of C_6H_5NC in methylcyclohexane was recorded at room temperature and is shown in Figure 5.4. The intensity of the $S_0 \rightarrow S_2$ transition was found to be much greater than the $S_0 \rightarrow S_1$ transition. Note that the solvent methylcyclohexane begins absorbing around 2200 Å. There is more structure in $S_0 \rightarrow S_1$ transition than in the $S_0 \rightarrow S_2$.

The fluorescence excitation spectrum of C_6H_5NC was taken at 77°K in 3-methylpentane and is shown in Figure 5.5. This spectrum was

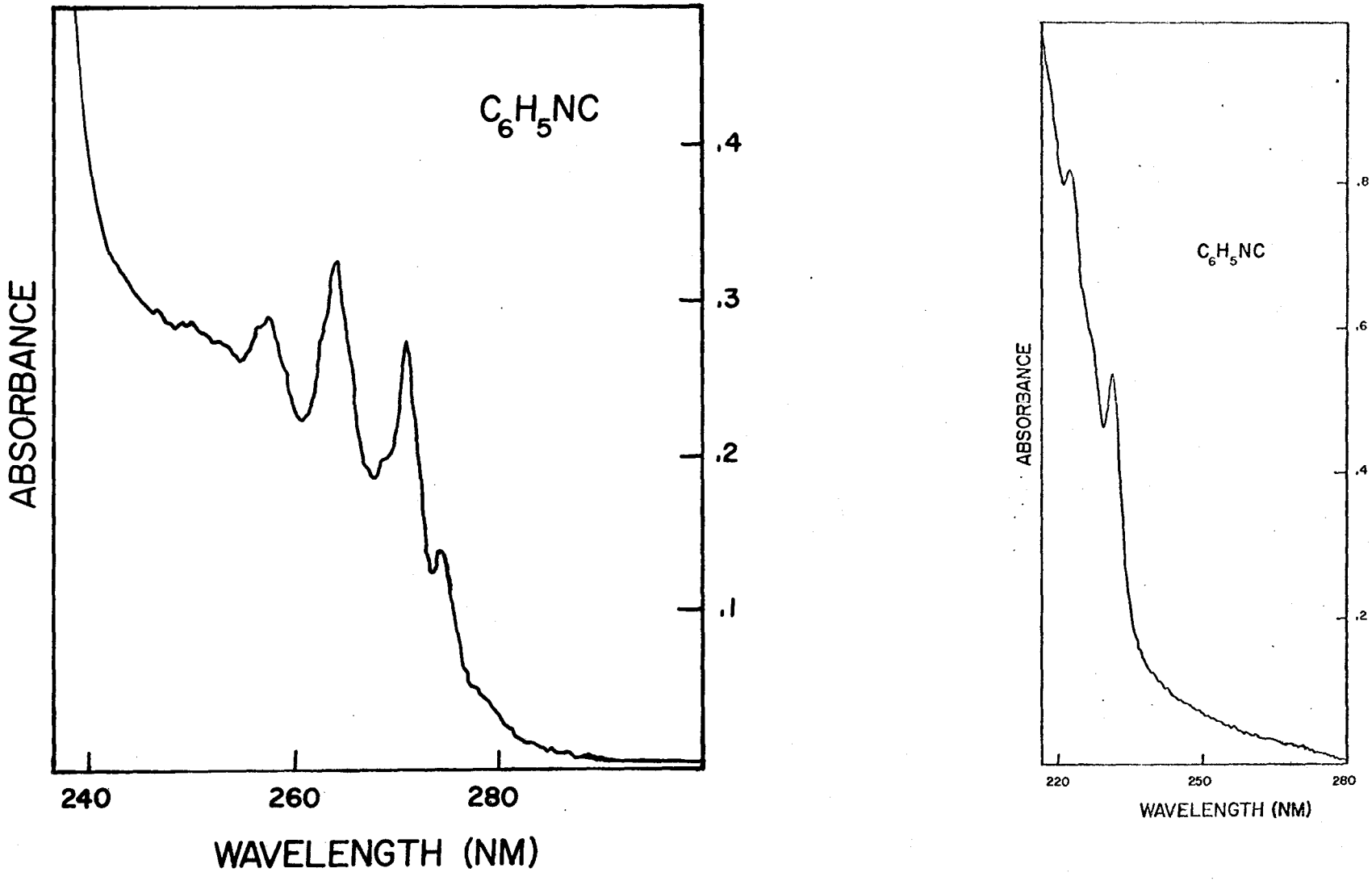

Figure 5.4 a Liquid electronic absorption of phenyl isocyanide in methylcyclohexane showing $S_0 \rightarrow S_1$ transition.
b Liquid electronic absorption of phenyl isocyanide in methylcyclohexane showing $S_0 \rightarrow S_2$ transition.

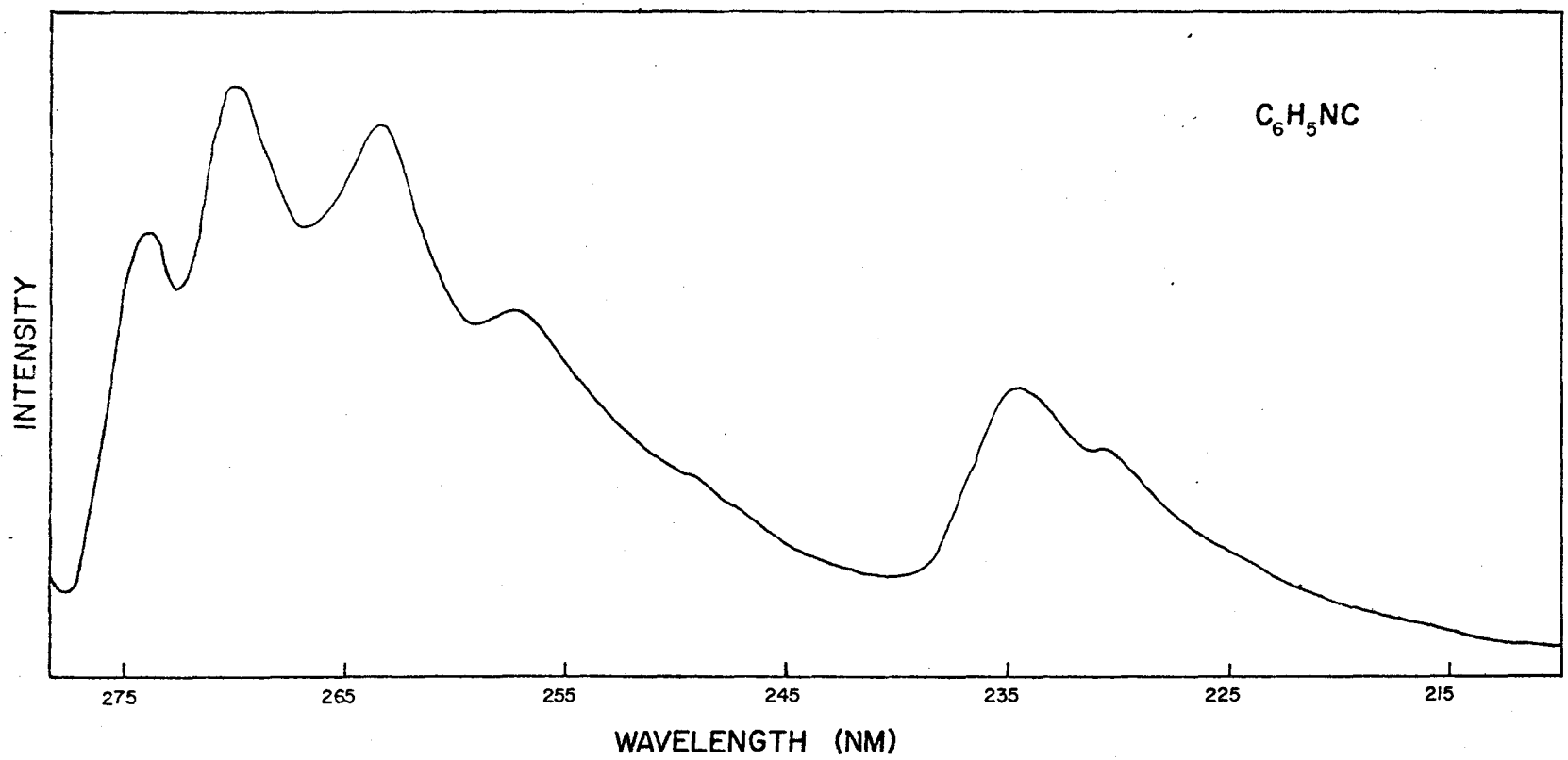

Figure 5.5 Fluorescence excitation of phenyl isocyanide in 3-methylpentane at 77°K.

obtained by monitoring a fluorescence band at 2979 Å and scanning the wavelength of the exciting light. Even though the spectrum shown is not accurately calibrated for wavelength or corrected for photomultiplier response, note that the general features of the liquid phase absorption spectrum of Figure 5.4 and the fluorescence excitation spectrum of Figure 5.5 are quite similar. This shows that the spectroscopic properties of C_6H_5NC in methylcyclohexane at room temperature do not differ appreciably when in a glass environment at 77°K, i.e., that perturbations and interactions in this glass environment are insignificant.

5.5 Fluorescence

The analysis of the fluorescence of C_6H_5NC and C_6D_5NC in 10^{-3} - 10^{-4} M polycrystalline methylcyclohexane at 77°K is listed in Tables 5.4 and 5.5. Typical spectra are shown in Figures 5.6 and 5.7. Spectra obtained with methylcyclohexane were sharper than those employing cyclohexane. In more concentrated solutions, a broad structureless band (probably eximer emission) appeared in the fluorescence region of C_6H_5NC and swamped out the luminescence normally found for 10^{-3} M concentrations and self-absorption of the (0,0) band took place. This is shown in Figure 5.8. With prolonged irradiation, the fluorescence intensity of dilute samples diminished greatly.

The fluorescence spectrum of C_6H_5NC in polycrystalline methylcyclohexane showed a splitting of the (0,0) and other prominent peaks

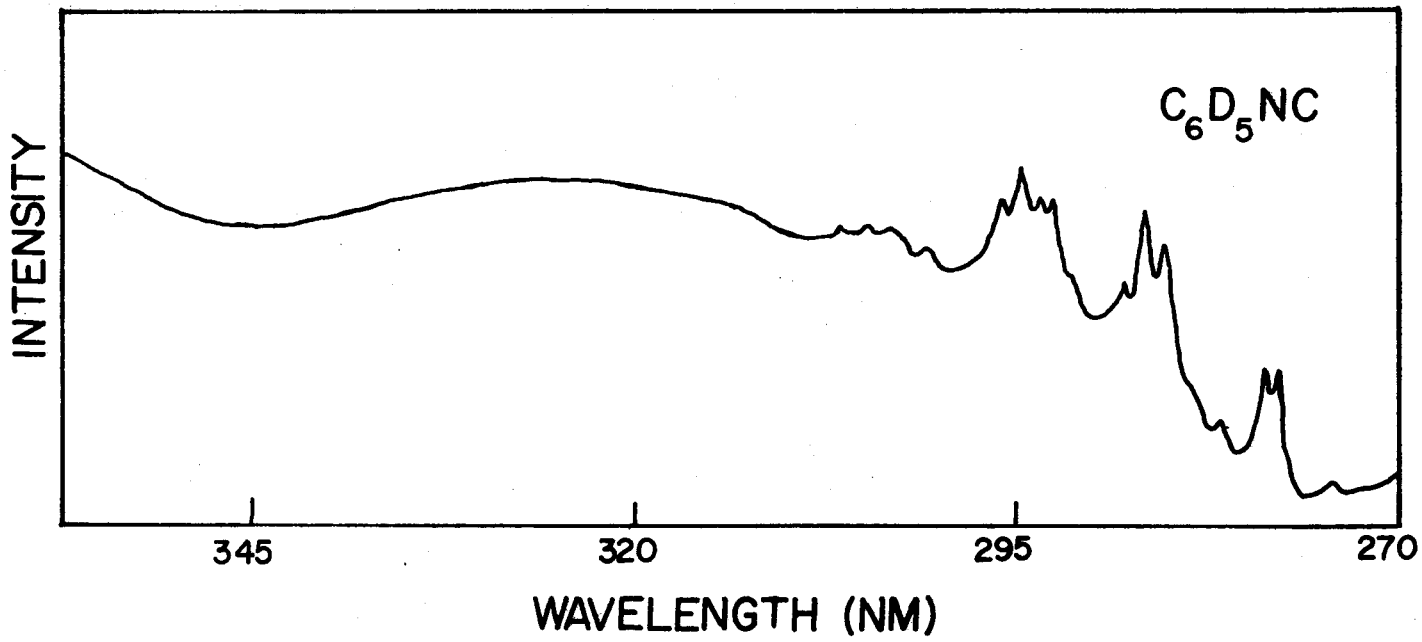

Figure 5.8 Eximer emission from concentrated solution of perdeuterophenyl isocyanide in cyclohexane at 77°K.

of 50 cm^{-1}. This is shown in Figure 5.9. The shape of the (0,0) and the other split bands was observed to vary. This is interpreted as emission due to two different orientations of C_6H_5NC in a single crystalline environment. Benzonitrile, C_6H_5CN also showed a splitting of the fluorescence in methylcyclohexane of 100 cm^{-1}. Significant variations in the shape of the (0,0) band with method of cooling was not observed for C_6H_5NC as was the case with C_6H_5CN.

The weak band at 36,415 cm^{-1} is assigned as the (0,0) transition. This band was found to have a value of 36,706 cm^{-1} in the gas phase electronic absorption spectrum of C_6H_5NC[13] and a value of 36,390 cm^{-1} in the liquid phase electronic absorption.

The medium intensity band at 1,015 cm^{-1} is assigned as the ring breathing mode, ν_{10}. The shoulder at 1165 cm^{-1} is assigned as ν_{29} with the medium band at 1190 being ν_7. The two strong bands at 485 cm^{-1} and 610 cm^{-1} are assigned as two nontotally symmetric b_2 vibrations, ν_{32} and ν_{31} respectively.

In the gas phase electronic absorption spectra of C_6H_5NC[13] some excited state frequencies are assigned as ν_7, ν_{10}, ν_{11}, ν_{31} and ν_{32}. Of these all are seen as ground state fundamentals in the fluorescence of C_6H_5NC except ν_{11}. The frequencies associated with their assignments seem reasonable based on what is found in the fluorescence of C_6H_5NC. Another common feature of the gas phase work with the fluorescence of C_6H_5NC is that ν_{10} is the most prominent frequency and most of the observed bands are based on one quantum of nontotally symmetric b_2 fundamentals which act as false origins at 452 cm^{-1} and 547 cm^{-1} in the excited state.

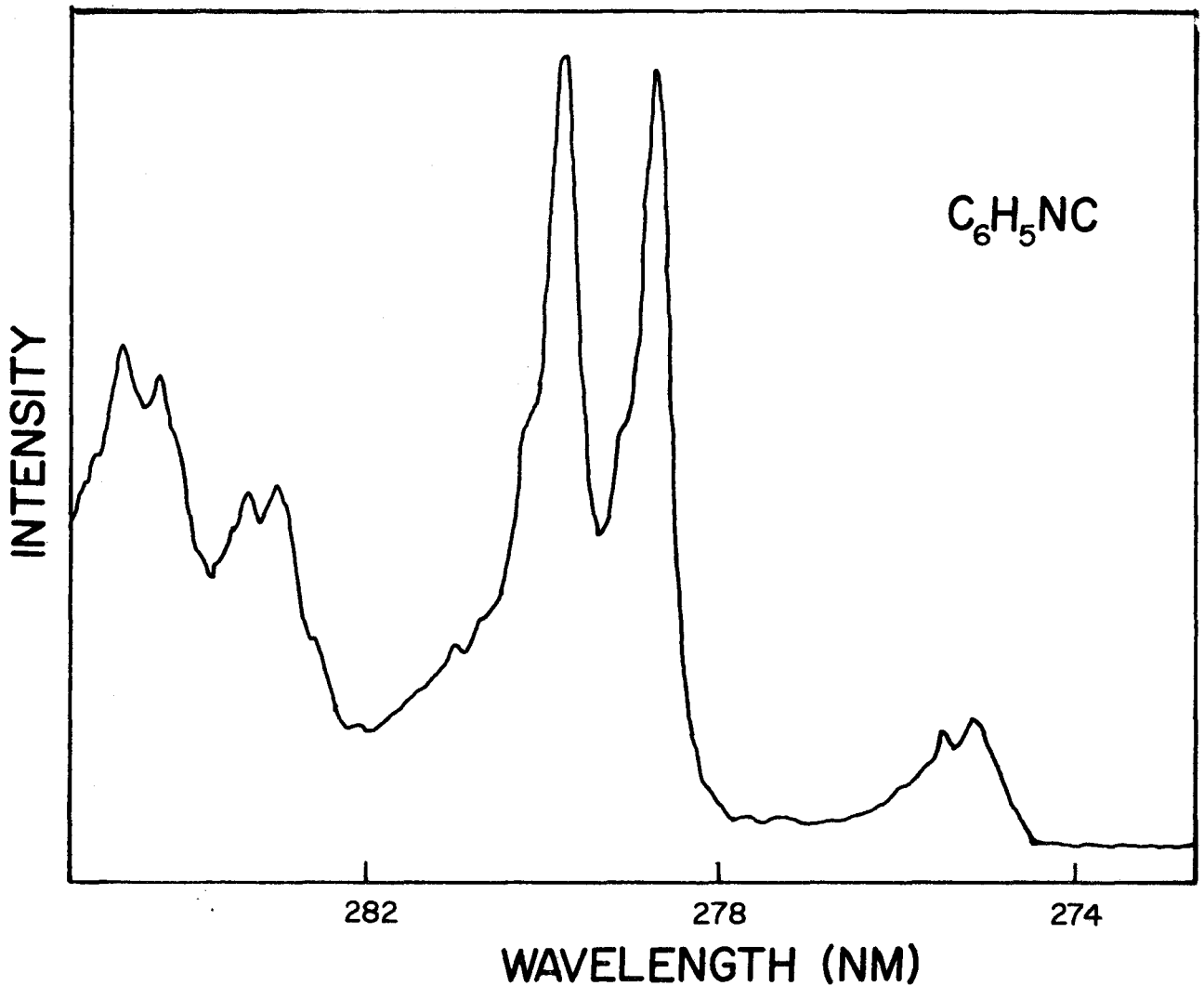

Figure 5.9 Fluorescence spectrum of phenyl isocyanide in polycrystalline methylcyclohexane at 77°K showing splitting of (0,0) and other prominent bands.

This was also found to be true in the fluorescence spectrum of C_6H_5NC as most of the spectrum is built on one quantum of the two false origins at 485 cm^{-1} and 610 cm^{-1} in the ground state.

The fluorescence of C_6D_5NC closely resembles that of C_6H_5NC. The (0,0) and all prominent bands are split by 40 cm^{-1}. All of the fundamentals seen in the fluorescence of C_6H_5NC are observed for C_6D_5NC except ν_{29}. These fundamentals ν_{32}, ν_{31}, ν_{10}, and ν_7 appear at 465 cm^{-1}, 595 cm^{-1}, 965 cm^{-1}, and 1142 cm^{-1} respectively. Again, one observes the two strong forbidden b_2 vibrations and the weak (0,0). Most of the bands are based on one quantum of nontotally symmetric b_2 fundamentals. The main progressions are in ν_{10} and ν_7 as was the case for C_6H_5NC.

Since the main progressions in the fluorescence of C_6H_5NC and C_6D_5NC are in the ring breathing mode, ν_{10}, and the X-sens (stretching of the ring and the -NC group) mode, ν_7, then the geometry of the lowest excited singlet state is believed to be that of a slightly expanded but still regular hexagon ring with a C-NC bond length which differs from that of the ground state. In the case of C_6H_5CCH the bond length of C-CCH was found to be contracted in the first excited singlet state relative to the ground singlet state[4].

The two nontotally symmetric b_2 vibrations appearing in the fluorescence spectra are symmetry forbidden by the integral shown in equation (2.24). This forbidden character introduced in the spectra by these two b_2 vibrations is customarily explained by invoking the Herzberg-Teller effect. The b_2 vibrations coupled to the electronic transition $S_0 \leftarrow S_1$ ($^1A_1 \leftarrow {}^1B_2$ in C_{2V}) mix in a large amount of the transition ($^1A_1 \leftarrow {}^1A_1$). The extent of mixing will be directly proportional to the mixing integral

and inversely proportional to the difference in energy of the perturbed and perturbing states.

If the latter is less than 1 ev then one will find the forbidden components to have an appreciable intensity[24]. Phenyl isocyanide has an energy difference of 0.83 ev between the first excited singlet state $^1B_2$ and the second excited singlet state $^1A_1$. Thus it is not surprising that the forbidden component in the fluorescence is much more strong than the (0,0) transition.

The fluorescence of C_6H_5NC with its two strong forbidden components and weak (0,0) is very similar to that of C_6H_5CCH[5] but very different from the fluorescence of C_6H_5CN[9]. The fluorescence of C_6H_5CN has a moderate (0,0) and the forbidden components appear very weakly.

A number of approaches may be taken to explain this behaviour among the three isoelectronic molecules cited above. The extent of vibronic coupling is inversely proportional to the energy differences between the perturbed and perturbing electronic states. In this respect C_6H_5CN[55] has a considerably bigger difference (1.04 ev) than either C_6H_5NC (0.83 ev) or C_6H_5CCH (0.75 ev)[56,57] and this correlates quite well with the extent of vibronic coupling. The amount of mixing of the two states depends linearly on the perturbation matrix element.

Albrecht[58] has tried to correlate the magnitude of the perturbation matrix element with the amount of charge transfer possessed by the first excited $^1B_2$ state in some substituted benzenes and the perturbing $^1A_1$ state. He found that two states which are largely non-charge-transfer give a large matrix element. The matrix element is small between a state

that is charge transfer and one that is not. If both states are charge transfer then no general predictions are possible. However, the amount of charge transfer possessed by these states in C_6H_5NC has not been calculated and thus no predictions may be made.

The change in dipole moment upon excitation, $\Delta\mu$, has been found by (13) to be directly proportional to the percentage of allowed character in vibronic transitions. It is felt by (13) that the change in $\Delta\mu$ can be directly related to the net extent of intramolecular charge transfer occurring on excitation and depends almost entirely on the π-electron distribution in the molecule. The quantity $\Delta\mu$ is thus a measure of the π-electron interaction between the ring and the substituent. They feel that their results are consistent with Albrecht's predictions if it is assumed the perturbing $^1A_1$ state does not have large amounts of charge transfer character and does not vary much from compound to compound. The value of $\Delta\mu$ for C_6H_5NC is 0.13 with 25% allowed character. For C_6H_5CCH $\Delta\mu$ is 0.14 with 25% allowed character. In the case of C_6H_5CN the corresponding values are 0.31 and 80%.

Brand and Knight[59] have interpreted changes in the moments of inertia $\Delta I_b = I_{b'} - I_{b''}$ in the $^1A_1 \rightarrow {}^1B_2$ transitions of some substituted benzenes in terms of charge transfer between the ring and the substituent.

King and van Putten[60] have looked at the transition $^1A_1 \rightarrow {}^1B_2$ for C_6H_5CCH and C_6H_5CN and have interpreted both $\Delta\mu$ and ΔI_b on excitation by looking in more detail at the molecular orbitals involved in charge transfer from the ring to the substituent and vice versa.

The fluorescence of benzene shows one strong forbidden component at $\tilde{\nu}$ 600 cm^{-1} in rigid solutions[32,61]. The main progression is in the ring breathing mode. The amount of forbidden character in monosubstituted benzenes will be a function of the net change brought about by the substituent on the π-electron system of the ring upon excitation. Evidently, the substituent -CN does have a net effect of perturbing the ring electrons quite significantly while -NC and -CCH do not. Thus the substituents -NC and -CCH although dissimilar chemically, produce quite similar spectra when acting as monosubstituents for benzene.

Figure 5.6

Fluorescence spectrum of phenyl isocyanide in polycrystalline methylcyclohexane at 77°K

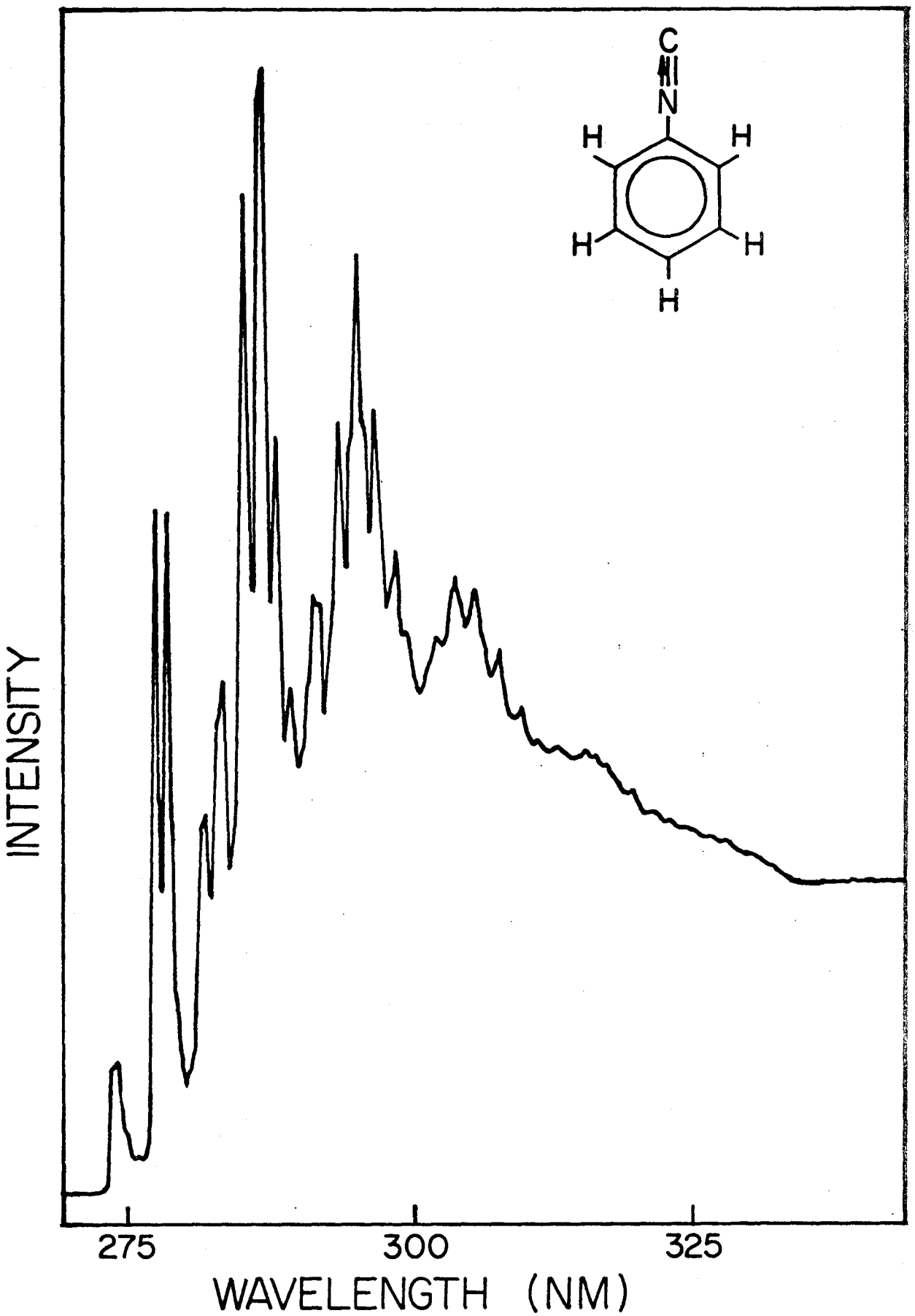
C
N
H
H
H
H
H
INTENSITY
275
300
325
WAVELENGTH (NM)

TABLE 5.4

Vibrational Analysis of the Fluorescence Spectrum of 10^{-3} M C_6H_5NC In Polycrystalline Methylcyclohexane at 77°K

Intensity[a]	Position[b]		Δν (cm^{-1})	Assignment[c]
	λ(nm x 10)	ν (cm^{-1})		
w	2746	36,415	0	$0'^{e}$,0
w	2750	36,365	50	$0''^{e}$,0
s	2783	35,930	485	0', ν_{32}
m	2787 sh[d]	35,880	535	0'', ν_{32}
s	2793	35,805	610	0', ν_{31}
m	2797 sh	35,755	660	0'', ν_{31}
m	2825	35,400	1015	0', ν_{10}
m	2829	35,350	1065	0'', ν_{10}
m	2837 sh	35,250	1165	0', ν_{29}
m	2839	35,225	1190	0', ν_{7}
m	2843	35,175	1240	0'', ν_{7}
vw	2855	35,025	1390	0', $\nu_{11}+\nu_{31}$
vs	2862	34,940	1475	0', $\nu_{10}+\nu_{32}$
m	2867 sh	34,880	1535	0'', $\nu_{10}+\nu_{32}$
vs	2875 sh	34,785	1630	0', $\nu_{10}+\nu_{31}$
vs	2877	34,760	1655	0', $\nu_{7}+\nu_{32}$
m	2882 sh	34,700	1715	0'', $\nu_{7}+\nu_{32}$
m	2890	34,600	1815	0', $\nu_{7}+\nu_{31}$
m	2893 sh	34,565	1850	0'', $\nu_{7}+\nu_{31}$
vw	2901	34,470	1945	0', $\nu_{7}+\nu_{11}$
vw	2904	34,435	1980	0'', $\nu_{7}+\nu_{11}$
vvw	2906	34,410	2005	0', $2\nu_{10}$
w	2911	34,350	2065	0'', $2\nu_{10}$
w	2923	34,210	2205	0', $\nu_{7}+\nu_{10}$
w	2928	34,155	2260	0'', $\nu_{7}+\nu_{10}$
m	2940 sh	34,015	2400	0', $2\nu_{7}$

Table 5.4 (contd)

Intensity[a]	Position[b]		Δν (cm^{-1})	Assignment[c]
	λ(nm x 10)	ν (cm^{-1})		
m	2946	33,945	2470	0', $2\nu_{10}+\nu_{32}$
m	2963	33,750	2665	0', $\nu_7+\nu_{10}+\nu_{32}$
m	2966 sh	33,715	2700	0", $\nu_7+\nu_{10}+\nu_{32}$
m	2979	33,570	2845	0', $2\nu_7+\nu_{32}$
vw	2993	33,410	3005	0', $3\nu_{10}$
vw	2997	33,365	3050	0", $3\nu_{10}$
vvw	3008	33,245	3170	0', $\nu_7+2\nu_{10}$
vw	3038	32,915	3500	0', $3\nu_{10}+\nu_{32}$
w	3050	32,785	3630	0', $\nu_7+2\nu_{10}+\nu_{32}$
w	3071	32,565	3850	0', $2\nu_7+\nu_{10}+\nu_{32}$
vw	3091	32,350	4065	0', $3\nu_7+\nu_{32}$
vvw	3107	32,185	4230	0', $\nu_7+3\nu_{10}$

a Uncorrected for instrumental response: s = strong, m = medium, w = weak, v = very.

b Error about ± 0.1 nm.

c Numbering of the normal modes follows Herzberg.

d sh = shoulder

e 0' and 0" refer to the vibrationless levels of the first excited singlet state of the phenyl isocyanides in two different orientations.

Figure 5.7

Fluorescence spectrum of perdeuterophenyl isocyanide in polycrystalline methylcyclohexane at 77°K

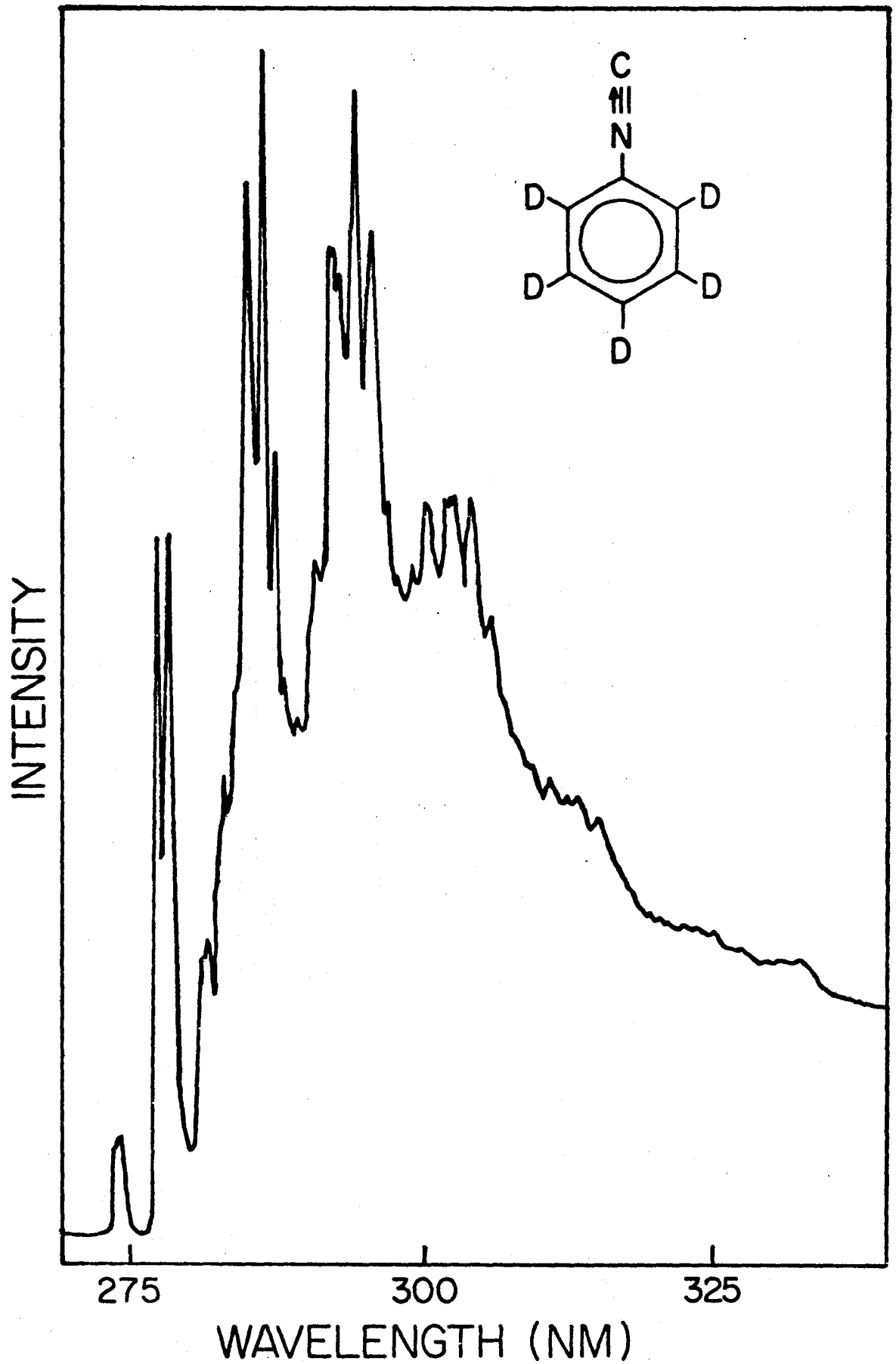
C
N
D
D
D
D
D
INTENSITY
275
300
325
WAVELENGTH (NM)

TABLE 5.5

Vibrational Analysis of the Fluorescence Spectrum of 10^{-3} M C_6D_5NC in Polycrystalline Methylcyclohexane at 77°K

Intensity	Position[b]		$\Delta\nu$ (cm^{-1}	Assignment[c]
	λ(nm x 10)	ν (cm^{-1})		
w	2735	36,565	0	$0'^{e}$,0
w	2738	36,525	40	$0''^{e}$,0
s	2770	36,100	465	0', ν_{32}
m	2773 sh	36,060	505	0'', ν_{32}
s	2780	35,970	595	0', ν_{31}
m	2783 sh	35,930	635	0'', ν_{31}
w	2809	35,600	965	0', ν_{10}
w	2813	35,550	1015	0'', ν_{10}
w	2823 sh	35,425	1140	0', ν_{7}
w	2826	35,385	1180	0'', ν_{7}
w	2834 sh	35,285	1280	0', ν_{27}
w	2836 sh	35,260	1305	0', $\nu_{11}+\nu_{31}$
s	2845	35,150	1415	0', $\nu_{10}+\nu_{32}$
m	2849 sh	35,100	1465	0'', $\nu_{10}+\nu_{32}$
s	2856 sh	35,015	1550	0', $\nu_{10}+\nu_{31}$
s	2859	34,975	1590	0', $\nu_{7}+\nu_{32}$
m	2863 sh	34,930	1635	0'', $\nu_{7}+\nu_{32}$
m	2870	34,845	1720	0', $\nu_{7}+\nu_{31}$
w	2874 sh	34,795	1770	0'', $\nu_{7}+\nu_{31}$
vw	2879	34,735	1830	0', $\nu_{7}+\nu_{11}$
vvw	2885	34,660	1905	0', $2\nu_{10}$
vvw	2890	34,600	1965	0'', $2\nu_{10}$
w	2901 sh	34,470	2095	0', $\nu_{7}+\nu_{10}$
w	2905	34,425	2140	0'', $\nu_{7}+\nu_{10}$
m	2917	34,280	2285	0', $2\nu_{7}$
m	2920	34,245	2320	0'', $2\nu_{7}$

Table 5.5 (contd)

Intensity	Position[b]		$\Delta\nu$ (cm^{-1})	Assignment[c]
	λ(nmx10)	ν (cm^{-1})		
m	2925	34,190	2375	0', $2\nu_{10}+\nu_{32}$
m	2928 sh	34,155	2410	0", $2\nu_{10}+\nu_{32}$
m	2936 sh	34,060	2505	0', $2\nu_{10}+\nu_{31}$
s	2939	34,025	2540	0', $\nu_7+\nu_{10}+\nu_{32}$
m	2951	33,885	2680	0', $\nu_7+\nu_{10}+\nu_{31}$
w	2967	33,705	2860	0', $2\nu_7+\nu_{31}$
vw	2978	33,580	2985	0', $2\nu_7+\nu_{11}$
vw	2987	33,480	3085	0', $\nu_7+2\nu_{10}$
w	2999	33,345	3220	0', $2\nu_7+\nu_{10}$
w	3003	33,300	3265	0", $2\nu_7+\nu_{10}$
w	3017	33,145	3420	0', $3\nu_7$
w	3021	33,100	3465	0", $3\nu_7$
w	3027	33,035	3530	0', $\nu_7+2\nu_{10}+\nu_{32}$
w	3040	32,895	3670	0', $\nu_7+2\nu_{10}+\nu_{31}$
vw	3055	32,735	3830	0', $2\nu_7+\nu_{10}+\nu_{31}$
vvw	3092	32,340	4225	0', $2\nu_7+2\nu_{10}$
vvw	3105	32,205	4360	0', $3\nu_7+\nu_{10}$
vvw	3133	31,920	4645	0', $2\nu_7+2\nu_{10}+\nu_{32}$
vvw	3148	31,765	4800	0', $2\nu_7+2\nu_{10}+\nu_{31}$

a Uncorrected for instrumental response: s = strong, m = medium, w = weak, v = very.
b Error about $\pm$ 0.1 nm
c Numbering of the normal modes follows Herzberg
d sh = shoulder
e 0' and 0" refer to the vibrationless levels of the first excited singlet state of the phenyl isocyanides in two different orientations

CHAPTER VI

SUMMARY

Infrared and Raman spectra of liquid phenyl isocyanide and perdeuterophenyl isocyanide were recorded and frequencies were assigned to the 33 normal modes of vibration.

Vibrational analyses of the fluorescence and phosphorescence spectra of phenyl isocyanide and perdeuterophenyl isocyanide in polycrystalline methylcyclohexane at 77°K were performed. The fluorescence spectra showed splittings of 50 cm^{-1} for C_6H_5NC and 40 cm^{-1} for C_6D_5NC and were attributed to two different orientations of the solute molecules in a single crystalline environment. The phosphorescence spectra showed no splittings.

The vibrational analyses of the phosphorescences are consistent with a planar, non-hexagonal ring triplet state geometry and that of the fluorescences consistent with a planar, slightly expanded ring excited singlet state geometry with a change in the ring-substituent group C-NC bond distance from that of the ground state.

The lowest triplet state orbital symmetry is assigned as $^3A_1$ on the basis of polarization measurements of the phosphorescence (0,0) band.

REFERENCES

1. D. P. Craig, J. Chem. Soc., 2146 (1950).
2. J. B. Coon, R. E. DeWames, and C. M. Loyd, J. Mol. Spectrosc., 8, 285 (1962).
3. G. C. Neiman, J. Chem. Phys., 50, 1674 (1969).
4. G. W. King and S. P. So, J. Mol. Spectrosc., 36, 468 (1970).
5. H. Singh and J. D. Laposa, J. Luminescence, 5, 32 (1972).
6. H. Singh and J. D. Laposa, J. Luminescence, 3, 287 (1971).
7. J. H. S. Green, Spectrochim. Acta., 17, 609 (1961).
8. R. J. Jakobsen, Spectrochim. Acta., 21, 127 (1965).
9. G. L. LeBel and J. D. Laposa, J. Mol. Spectrosc., 41, 249 (1972).
10. S. Leach and R. Lopez-Delgado, J. Chem. Phys., 61, 1636 (1964).
11. M. S. deGroot and J. H. van der Waals, Mol. Phys., 6, 545 (1963).
12. G. C. Neiman and D. S. Tinti, J. Mol. Spectrosc., 46, 1432 (1967).
13. A. R. Muirhead, A. Hartford, K. T. Huang, and J. R. Lombardi, J. Chem. Phys., 56, 4385 (1972).
14. K. L. Wolf and O. Strasser, Z. Physik. Chem., B21, 389 (1933).
15. I. Ugi and R. Meyr, Chem. Ber., 93, 239 (1960).
16. R. S. Mulliken, J. Chem. Phys., 23, 1997 (1955).
17. Gerald W. King, Spectroscopy and Molecular Structure, p. 113, Holt, Rinehart and Winston, Inc., New York, 1964.
18. M. Born and R. Oppenheimer, Ann. d. Physik., 84, 457 (1927).
19. G. Herzberg, Infrared and Raman Spectra, Van Nostrand, Princeton, New Jersey, 1945.

20. E. B. Wilson, J. C. Decius and P. C. Cross, Molecular Vibrations, McGraw-Hill, New York, 1955.

21. H. A. Szymanski, editor, Raman Spectroscopy, Plenum Press, New York, 1967.

22. T. R. Gilson and P. J. Hendra, Laser Raman Spectroscopy, Wiley-Interscience, New York, 1970.

23. J. N. Murrell, The Theory of Electronic Spectra of Organic Molecules, John Wiley and Sons Inc., New York, 1963.

24. G. Herzberg, Electronic Spectra of Polyatomic Molecules, Van Nostrand, Princeton, 1966.

25. G. Herzberg and E. Teller, Z. Physik. Chem., B21, 410 (1933).

26. M. Kasha, Discussions Faraday Soc., 9, 14 (1950).

27. M. Kasha, Radiation Res., Suppl. 2, p. 243 (1960).

28. G. W. Robinson, J. Mol. Spectrosc., 6, 58 (1961).

29. G. W. Robinson and R. P. Frosch, J. Chem. Phys., 37, 1962 (1962).

30. G. W. Robinson and R. P. Frosch, J. Chem. Phys., 38, 1187 (1963).

31. B. Meyer, Low Temperature Spectroscopy, American Elsevier Publishing Company, Inc., New York, 1971.

32. J. D. Spangler and N. G. Kilmer, J. Chem. Phys., 48, 698 (1968).

33. C. A. Parker, Photoluminescence of Solutions, Elsevier Publishing Company, New York, 1968.

34. A. C. Albrecht, J. Mol. Spectrosc., 6, 84 (1961).

35. D. S. McClure, J. Chem. Phys., 17, 665 (1949).

36. J. U. Nef, Ann. Chem., 270, 309 (1892).

37. I. Ugi and R. Meyr, Organic Syntheses, 41, 101 (1961).

38. R. G. Bell and C. Chan, unpublished results.

39. R. R. Randle and D. H. Whiffen, Molecular Spectroscopy Conference held by the Institute of Petroleum, London, 1955.

40. J. K. Wilmshurst and H. J. Bernstein, Can. J. Chem., 35, 911 (1957).

41. F. A. Andersen, B. Bak, S. Brodersen and J. Rastrup-Andersen, J. Chem. Phys., 23, 1047 (1955).

42. D. H. Whiffen, Spectrochimica Acta., 7, 253 (1955).

43. D. H. Whiffen, J. Chem. Soc., 1350 (1956).

44. K. S. Pitzer and D. W. Scott, J. Am. Chem. Soc., 65, 824 (1943).

45. J. C. Evans, Spectrochim. Acta., 16, 428 (1960).

46. R. A. Nalepa and J. D. Laposa, to appear in J. Luminescence.

47. G. Varsanyi, Vibrational Spectra of Benzene Derivatives, Academic Press, New York, 1969.

48. C. W. Young, R. B. DuVall and N. Wright, Anal. Chem., 23, 709 (1951).

49. P. D. Knight, Ph.D. Dissertation, Nanderbilt University (1971).

50. T. E. Martin and A. H. Kalantar, J. Chem. Phys., 49, 244 (1968).

51. D. F. Evans, J. Chem. Soc., 2753 (1959).

52. A. C. Ling and J. E. Willard, J. Phys. Chem., 72, 1918 (1968).

53. A. C. Ling and J. E. Willard, J. Phys. Chem., 72, 3349 (1968).

54. D. M. Haaland and G. C. Nieman, J. Chem. Phys., 59, 1013 (1973).

55. J. N. Murrell, Tetrahedron, 19, Suppl. 2, 277 (1963).

56. G. W. King and S. P. So, J. Mol. Spectrosc., 37, 543 (1971).

57. S. P. So, Thesis, McMaster University, 1969.

58. A. C. Albrecht, J. Chem. Phys., 33, 156 (1960).

59. J. C. D. Brand and P. D. Knight, J. Mol. Spectrosc., 36, 328 (1970).

60. G. W. King and A. A. G. van Putten, J. Mol. Spectrosc., 44, 286 (1972).

61. P. G. Russell and A. C. Albrecht, J. Chem. Phys., 41, 2536 (1964).

62. E. B. Wilson, Phys. Rev., 45, 706 (1934).

63. W. D. Mross and G. Zundel, Spectrochim. Acta., 26A, 1097 (1970).